Minimizing Embodied Carbon in Multi-Material Structural Optimization of Planar Trusses

by
Brenda G. Stern

B.S. Civil and Environmental Engineering
Massachusetts Institute of Technology, 2017

SUBMITTED TO THE DEPARTMENT OF CIVIL AND ENVIRONMENTAL ENGINEERING IN PARTIAL FULFILLMENT OF THE REQUIREMENTS FOR THE DEGREE OF

MASTER OF ENGINEERING IN CIVIL AND ENVIRONMENTAL ENGINEERING
AT THE
MASSACHUSETTS INSTITUTE OF TECHNOLOGY

JUNE 2018

Signature of Author: Signature redacted
Department of Civil and Environmental Engineering
May 11, 2018

Certified by: Signature redacted
Caitlin T. Mueller
Assistant Professor of Architecture and Civil and Environmental Engineering
Thesis Supervisor

Accepted by: Signature redacted
Jesse Kroll
Professor of Civil and Environmental Engineering
Chair, Graduate Program Committee

Minimizing Embodied Carbon in Multi-Material Structural Optimization of Planar Trusses

by
Brenda G. Stern

Submitted to the Department of Civil and Environmental Engineering on May 11th 2018 in Partial Fulfilment of the Requirements for the Degree of Master of Engineering in Civil and Environmental Engineering

Abstract

In the built environment, there is a growing emphasis on sustainable, energy efficient design that reduces carbon emissions. However, until recently, most efforts have focused only on reducing operational carbon [1]. As a result, the carbon embodied in construction materials, especially in a building's structural system, is becoming a larger contributor to the total carbon impacts of a building. Material type and quantity are important in determining the extent of this contribution because both will affect the amount of carbon emitted from the material production. For example, two common materials for truss structures are timber and steel. While timber's embodied carbon coefficient ($kg_{CO2e}/kg_{material}$) and density are lower than that of steel, its much lower strength means that it may not always result in the least-emitting structural design. As a result, the choice of the more sustainable material for any given member is dependent on factors such as the truss span or shape. Multi-material structures offer a solution to create efficient structures with a lower environmental impact. In this thesis, an embodied carbon optimization investigates truss structures of various spans and studies how multi-material and single-material designs compare. This research introduces a new approach for multi-material designs for the optimization of embodied carbon and demonstrates the advantages of using structural optimization and multi-material designs for sustainability.

Keywords: Optimization, embodied carbon, sustainable structures, truss structures

Thesis Supervisor: Caitlin T. Mueller
Title: Assistant Professor of Architecture and Civil and Environmental Engineering

Acknowledgements

I would first like to extend my sincere appreciation for my thesis advisor, Professor Caitlin T. Mueller, for her encouragement and guidance. Her support and enthusiasm throughout my studies at MIT has been instrumental in the development of this research. I would also like to thank Dr. Catherine De Wolf for her advice and suggestions on the embodied carbon calculations. I am also thankful to the members of the Digital Structures research group for their valuable feedback and assistance.

I would like to thank all my fellow Masters of Engineering students, as well as other classmates, who have helped me get through the rough times and enjoy good times at MIT. I am grateful to have met such inspiring and passionate people whom I have learned so much from.

Finally, I would like to thank my family for their incredible support throughout my education. I could not have done it without you.

Table of Contents

List of Tables

List of Figures

1. Introduction

Buildings are a major contributor to global carbon emissions as a result of both operational energy and embodied energy. In 2016, the total building sector accounted for 39% of US energy consumption, shown in Figure 1 [2]. Although there is a growing emphasis on sustainable design in the built environment, until recently, most efforts focused only on reducing operational carbon. Operational carbon is the carbon emitted by the energy needed for heating, cooling, and lighting over the structure's life cycle [1]. As a result of improved operational performance, the embodied carbon, the carbon emitted from the production of construction materials, is becoming a larger contributor to the total carbon impacts of a building. This relationship is shown in Figure 2 [3]. Consequently, the decisions that structural engineers and designers make are having a larger effect on a building's environmental impact and thus, require more attention.

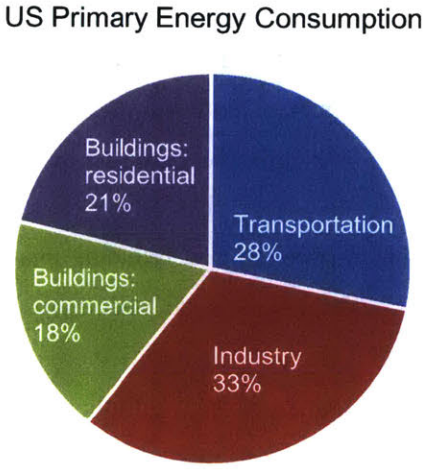

Figure 1: US Energy Consumption [2]

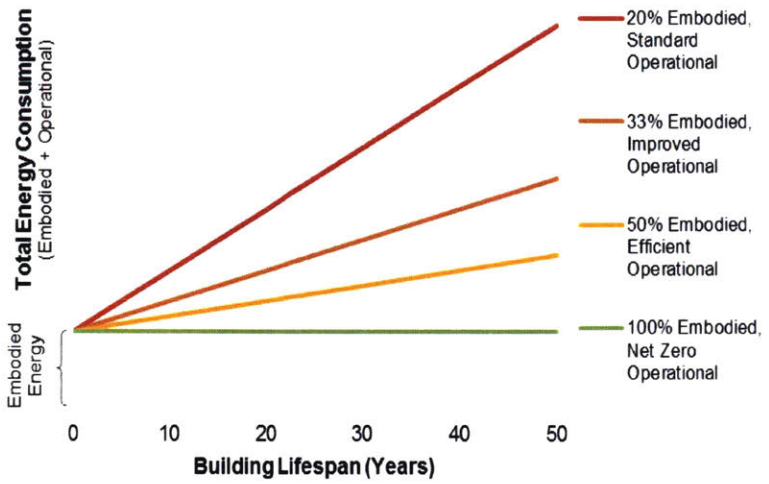

Figure 2: Total energy consumption over a building's lifespan based on the operational energy efficiency [3]

Specifically, material type and quantity are important in determining the extent of this contribution because both will affect the amount of carbon emitted from the material production. The embodied carbon in structures is measured by calculating the Global Warming Potential (GWP), which can be done through multiplying the structural material quantity, SMQ, by the appropriate embodied carbon coefficient, ECC. The SMQ is the weight of the structure normalized by span length, $kg_{material}/m$, and the ECC is a material-dependent value, calculated as the amount of carbon emitted per unit weight of the material, $kg_{CO2e}/kg_{material}$. The University of Bath's Inventory of Carbon and Energy (ICE) provides information on the ECC values for several materials [4]. In addition, instead of just one general value for each material, it includes specific ECC values based on properties such as strength and recycled content. This allows the user to select a more accurate value for their specific design. Timber, one of the materials listed, has variations in the ECC due to differences in carbon sequestration, engineered timber, sustainable forest management, end-of-life scenarios, provenance, and transport/availability [1]. Steel can vary due to recycled content, structural steel/rebar, energy mix, available scrap steel, and manufacturing process [1].

Structural optimization is a promising approach for reducing material usage and has been applied extensively since the 1960s in single-material trusses. The geometry of a truss affects how the forces are distributed through the different members and thus, the required cross-sectional area of each member. Two common materials for trusses are timber and steel. While timber's embodied carbon coefficient is lower than that of steel, its strength and density properties also play a role in calculating total carbon emissions, and it is not always the best choice. These properties are shown in Table 1 below. Figure 3 shows, through

an Ashby diagram, the relationship between the strength and the mass of CO_2 per cubic meter for many materials, including timber and steel.

Table 1: Material Values for Steel and Glulam (Glue Laminated Timber)

	ECC ($kg_{CO2e}/kg_{material}$)	E (kN/cm^2)	Fy (kN/cm^2)	Density (kg/m^3)
Steel	1.46 [4]	21000 [5]	20.7 [5]	7870 [6]
Glulam	0.42 [4]	800 [5]	0.7 [5]	570 [6]

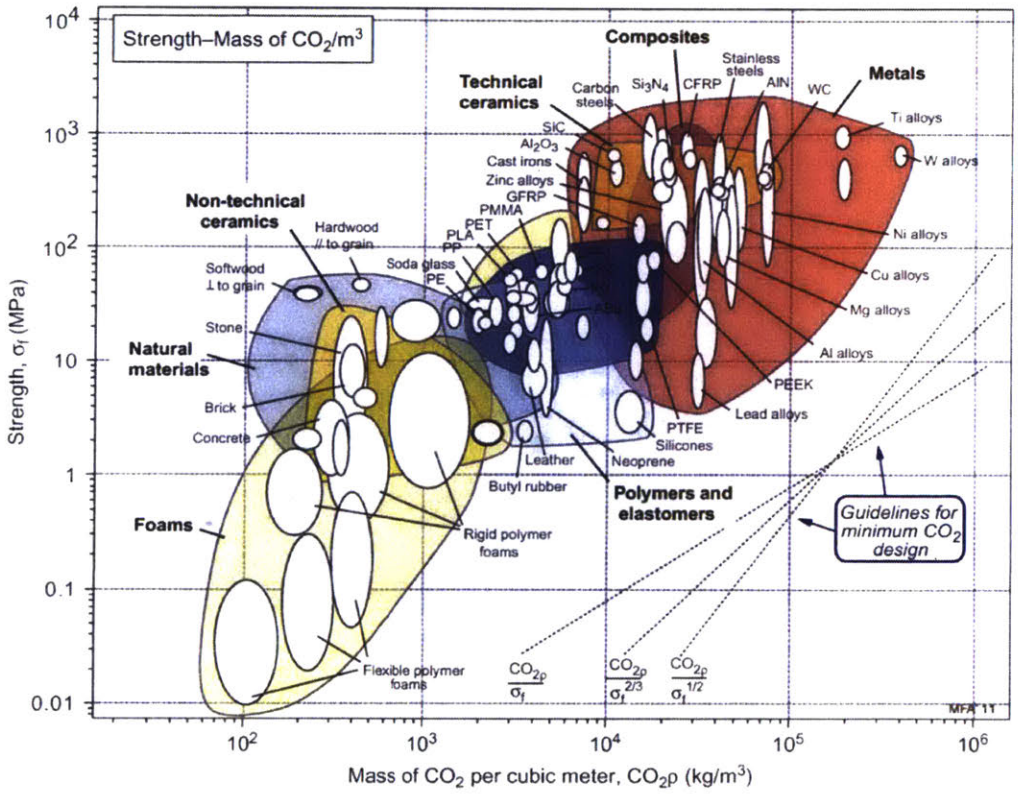

Figure 3: Ashby diagram: embodied carbon vs. strength [7]

As a result, the choice of the more sustainable material for any given member is dependent on factors such as truss span or shape. As such, allowing for multi-material structures during optimization offers the opportunity to find structurally efficient solutions with lower environmental impact than traditional single-material structures. The Scottish Parliament building in Figure 4 is an example of a large-scale multi-material roof truss, while Figure 5 shows a smaller scale structural system, an open web joist. Figure 6 is another roof truss example, the Depot designed by Bridgeport Design Group.

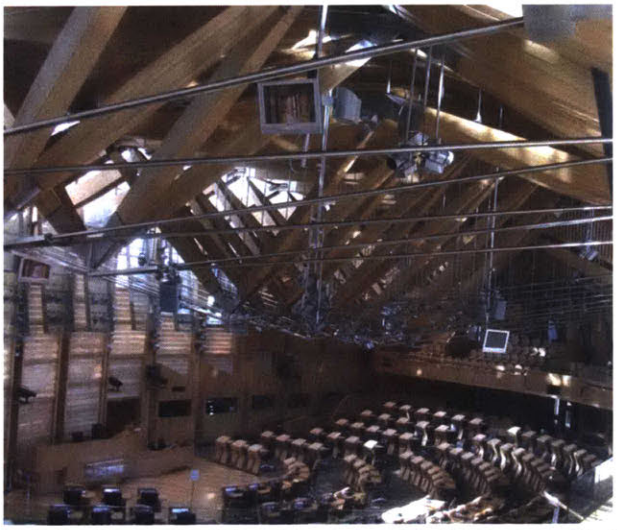

Figure 4: The Scottish Parliament building is an example of a steel and timber roof design [8]

Figure 5: An open web joist [9]

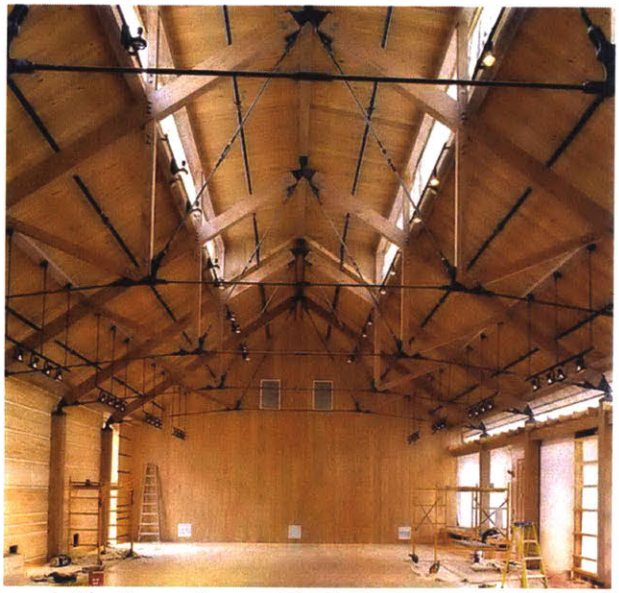

Figure 6: The Depot designed by Bridgeport Design Group [10]

2. Literature Review

This chapter reviews previous research that has been done on embodied carbon and structural optimization as well as case studies comparing different materials. The first section discusses embodied carbon benchmarking, the second section reviews specific case studies, and the third section reviews structural optimization research. While there has been previous work in all three areas, there has yet to be a comprehensive analysis at the intersection of the three. The final section discusses how this thesis will investigate this intersection between the three topics.

2.1 Overview of current work on embodied carbon in structures

This research builds upon a growing field of work in analyzing and reducing embodied carbon in buildings and comparing different construction materials. Currently, most embodied carbon research focuses on collecting data about materials and existing buildings. The Database of Embodied Quantity Outputs (deQo) collects information about the GWP of buildings and allows designers to compare their work against others [11]. When seeking a green building certification, it is often necessary to compare the new structure against a reference building [1]. Therefore, it is important to have a baseline for embodied carbon for various building types [1]. Though there is work done on benchmarking embodied carbon and analysis of existing buildings, there is less research on how to incorporate the results to structures still in the design phase.

2.2 Previous case studies comparing the environmental impacts of different materials

One case study comparing the environmental impacts of steel vs. glue laminated timber (glulam) was on the Raleigh-Durham Airport T2 Roof Truss, shown in Figure 7. An 86% GWP reduction was found for using glulam instead steel, in addition to improving other environmental impact categories [12]. This shows that, for some geometries, timber can be more sustainable than steel even with its lower strength. Trussoni *et al.* compared life cycle assessments for long span cable and truss structural systems [13]. One drawback in current engineering practice is that cost is the motivating factor, which often then translates to motivation to reduce material quantity. The greatest chance to improve the life cycle impacts of a building is during the design phase when the structural system is selected [13]. After this phase, reconsidering the structural system will increase the time and cost. The Inventory of Carbon and Energy was used during Trussoni *et al.*'s case study because of its accuracy, transparency, and comprehensive listing of structural materials [13]. In order for a complete comparison, the authors tried to keep the systems as equal as possible. They assumed that some things, such as construction necessities, were equal and were omitted from the comparison [13]. The authors analyzed the structures by comparing their mass and energy emissions. In some cases, they found that the heavier parts of the structural system were not the largest contributors to the carbon emissions [13]. This shows that structural design based on least weight may not lead to the most sustainable designs.

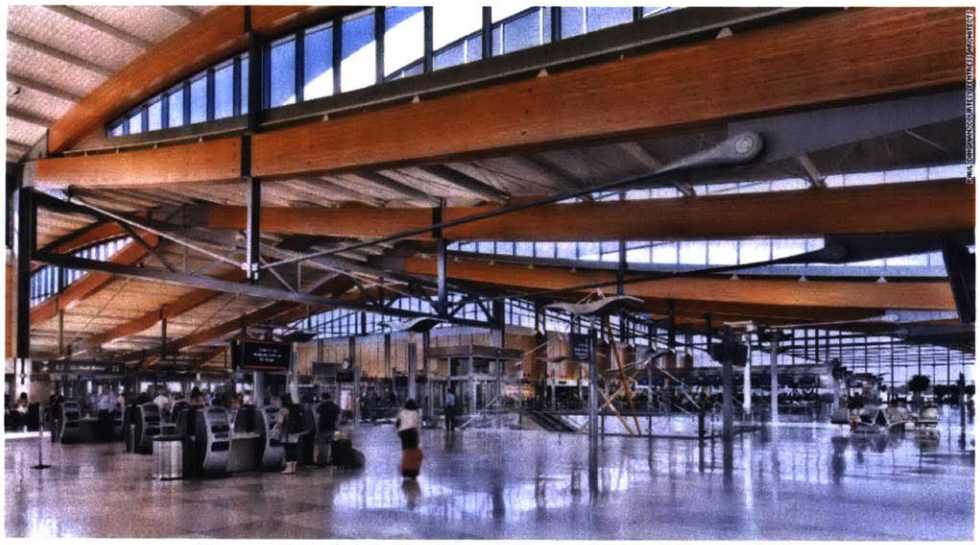

Figure 7: Raleigh-Durham Airport T2 Roof Truss [14]

2.3 Previous structural optimization research

Kripakaran *et al.* researched optimization for minimum cost design of trusses [15]. While structural optimization techniques have grown, many of these are for weight cost models [15]. Their optimization approach clusters types of members to decrease the number of different products [15]. This is because members of the truss that behave the same will most likely need the same product [15]. Their clusters were the top chord, bottom chord, and the two sets of diagonals [15]. Brown and Mueller used a multi-objective genetic algorithm for long span buildings to optimize embodied and operational energy in different cities for three different geometries [16]. However, the building material used for all optimizations was steel [16]. In contrast, Stolpe *et al.* investigated material-selection truss-topology optimization and showed that, at most, two materials are necessary for an optimal truss [17], which is the maximum number of materials this thesis will use. However, they did not investigate the environmental impact between the materials. In addition, they used yield stress to size both tension and compression members, even though buckling can cause failure first in compression members. Rakshit and Ananthasuresh investigated truss optimization for geometry and material selection, through they only used one material per geometry and used an extension of Ashby's method of material selection [18]. Some designers may choose the material first and then do structural optimization while others will choose the material based on a selected geometry. However, neither of these will necessarily find the best combination of both design variables. Optimizing both simultaneously can produce better results [18]. Their optimization study used stiffness, strength, and cost/weight as criteria for the design, but did not investigate the environmental impacts. Cazacu and Grama created a genetic algorithm in MATLAB to optimize the mass in steel truss structures under deflection and allowable stress constraints [19]. A fitness value is calculated based on the mass and conformity to stress and displacement constraints and then the designs are evolved towards a more optimal solution [19]. The parameters these researchers used include nodal positions, lengths of bars, areas of the bars, and diagonal bracing topology [19]. To abide by the constraints, a penalty function was designed that depends on the magnitudes of the violated constraints [19]. They created a test to see how well their algorithm, written in MATLAB, does by using their algorithm on a popular benchmark problem [19]. However, this research only uses one material and does not focus on sustainability implications.

2.4 Research aims

Though optimization has shown to be a useful tool to help building designers assess material choices, geometry, and environmental impacts, there has yet to be a study to analyze all three at once. This research aims to answer the following questions:

- Can multi-material designs perform better in terms of GWP compared to single-material designs?

- How much savings are possible due to shape optimization vs. material optimization?
- What is the best way to use steel and timber in long-span trusses to reduce embodied carbon?

These questions are addressed in the following chapters, which present analytical and numerical methods and results for multi-material structural optimization for GWP minimization.

3. Hand Calculation Analysis

In order to better understand how multi-material optimization works with an embodied carbon objective function, it is useful to begin with simple hand calculations. This chapter lays out the methods and outcomes of this process. This first section describes the values and equations used in this section. The next section investigates a simply supported triangular truss section and its results. The third section discusses a simply supported four-section rectangular truss and its results. It also includes a sensitivity analysis on the values used for the analysis. The final section discusses the key findings from these results.

3.1 Scope and assumptions

The first calculation method uses hand calculations and spreadsheets to find the GWP of two different truss shapes: a triangle and a four-section rectangle. The members of the trusses may be one of two materials: steel or timber. The steel cross sections are hollow tubes and the timber sections are solid squares. The wall thickness of the hollow tubes is kept constant as a ratio of the radius, shown in Figure 8. The tension members are sized based on allowable stress and the compression members are sized based on allowable stress and buckling. Assuming the forces in a given truss are known, the members can be sized accordingly, assuming continuous member sizes. This can be done by following the steps in Figure 8. With the cross-sectional area of the element known, it is multiplied by the length of the member, the material density, and the material ECC to obtain the total embodied carbon (kg_{CO2e}) for each element. Summing these values for

all members and dividing by the span length yields the GWP (kg_{CO2e}/m). Except for the sensitivity analysis in section 3.3.2, the material properties were constant as listed in Table 1. The steel assumes a 59% recycled amount [4]. The glulam assumes that the timber comes from a sustainable forest. Thus, the biomass can be considered carbon neutral so only the carbon derived from fossil fuel is included in the ECC value [4]. The timber does not include carbon sequestration. All ECC values are cradle to gate. Joints are not analyzed in this research.

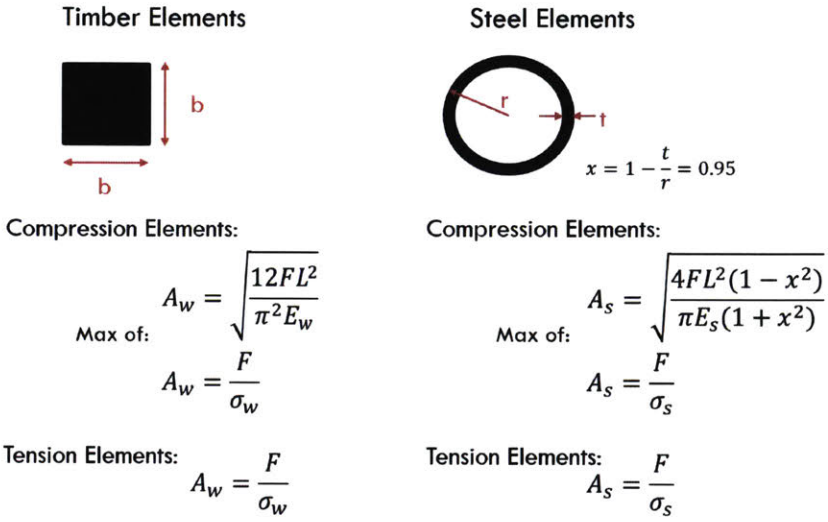

Figure 8: Cross section calculations

3.2 Triangular truss

3.2.1 Overview

The first shape analyzed is the simply supported triangular truss section shown in Figure 9. This truss assumes constant load P = 117kN and W = 10m, with the height, H, a variable. By varying the H/W ratio, the forces in the members can be found. Thus, it is possible to calculate the GWP as described in 3.1 for given materials. The diagonal members will always have the same material as one another, but not necessarily the same material as the bottom member. For this triangle design, the material combinations are written in the format "Diagonal-Bottom". For example, "g-s" means that the diagonal members are glulam and the bottom member is steel.

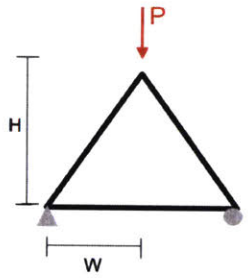

Figure 9: Triangle truss

3.2.2 Results

For the triangle truss, the diagonal members are in compression and the bottom member is in tension. Thus, the diagonal members are sensitive to buckling while the bottom member is only sized based on allowable stress. Figure 10 shows how increasing the *H/W* ratio changes the GWP for the four material combinations. When *H/W* is low, each of the material combinations is unique and dependent on both types of members. As *H/W* increases, these material combinations group into two main clusters, depending on the diagonal (compression) members. Whether the bottom (tension) member is steel or glulam makes little difference in the GWP. The required areas for each member based on the material when $H/W = 1$ are shown in Figure 11. Figure 12 and Figure 13 show the weight ($kg_{material}$) and embodied carbon (kg_{co2e}), respectively, for each member based on these required areas. Even though glulam has a lower density than steel, it has a significantly larger required cross sectional area. This results in the glulam member being heavier than the steel option for both member types. However, glulam also has a significantly lower ECC value than steel and this results in a lower embodied carbon. When comparing the two member types, the area and weight of the glulam diagonal members are much higher than that of the bottom member for either material. As a result, the embodied carbon for the diagonal member is greater than that for the bottom member, regardless of material. For the diagonal member, there is a larger difference in the embodied carbon based on the material. Thus, the diagonal member becomes the controlling factor for the clusters in Figure 10.

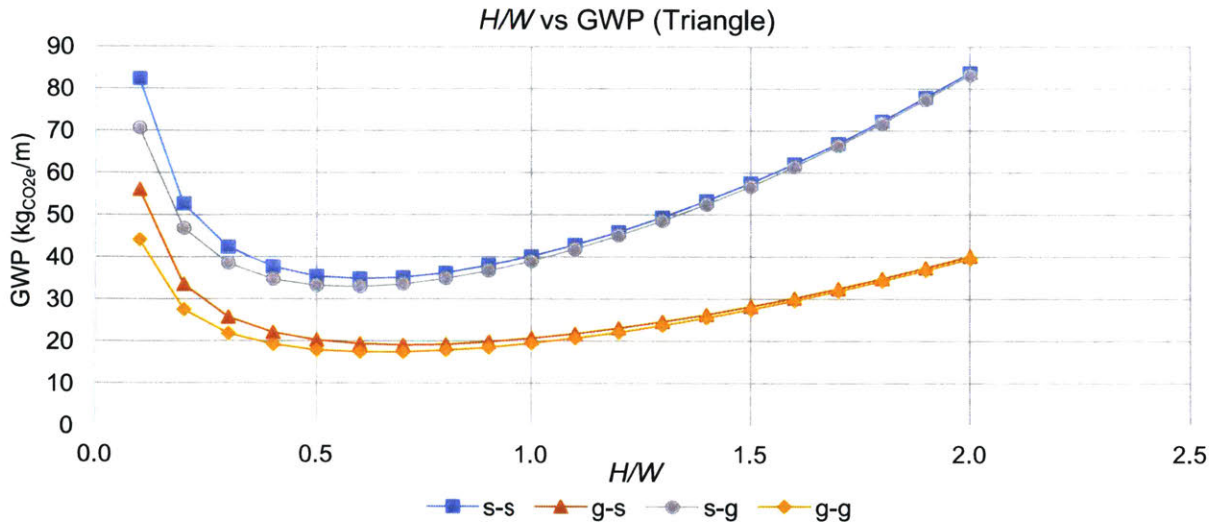

Figure 10: H/W vs GWP for the triangle truss (Material Order: Diagonal-Bottom)

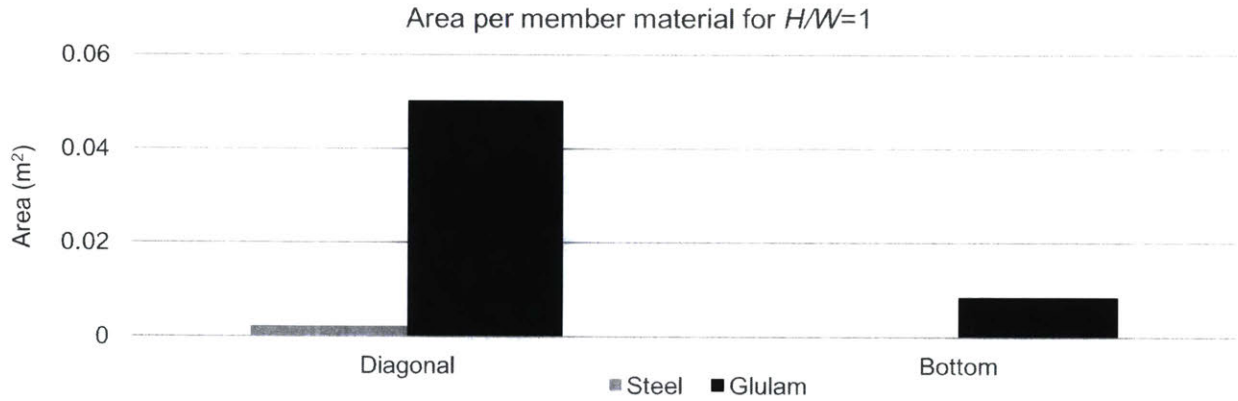

Figure 11: The area of each member for the triangle truss based on the material

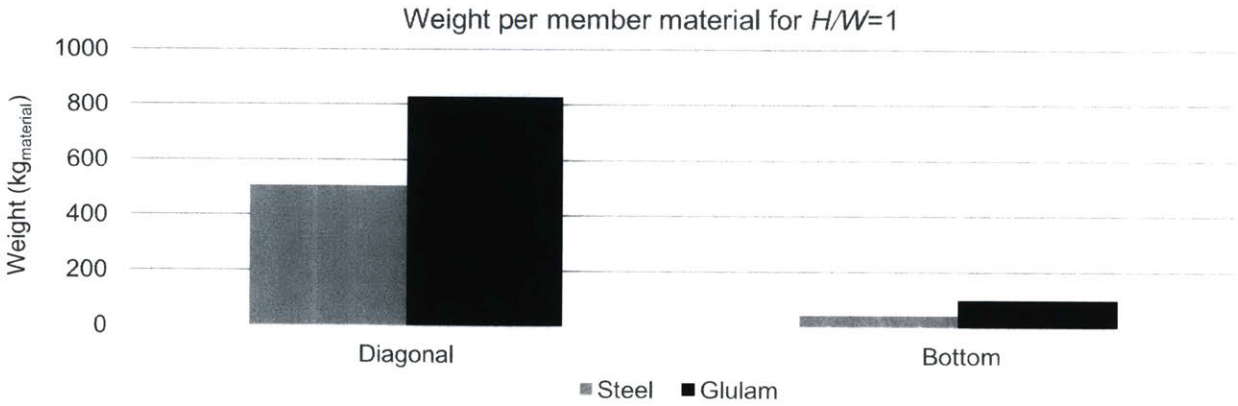

Figure 12: The weight of each member for the triangle truss based on the material

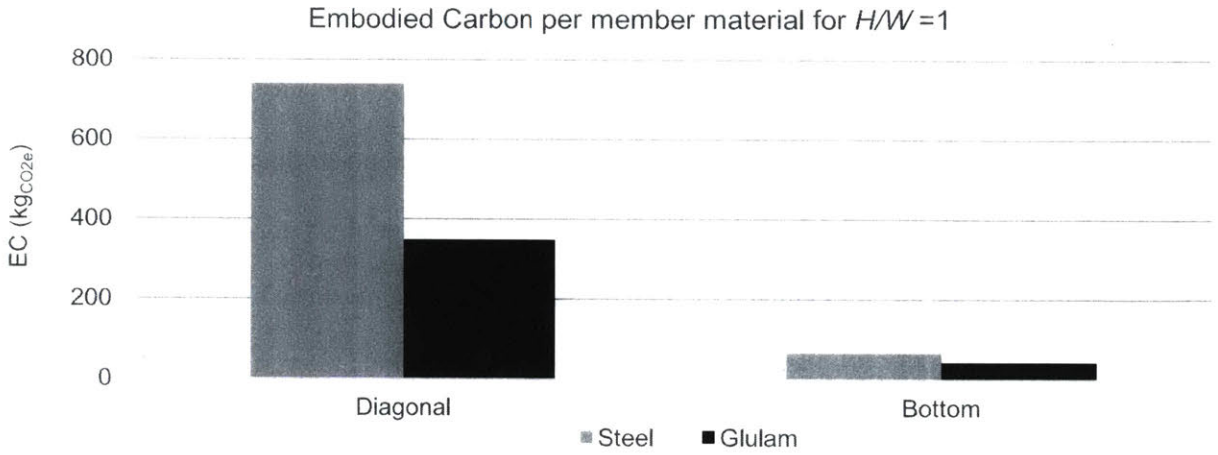

Figure 13: The embodied carbon of each member for the triangle truss based on the material

3.3 Standard rectangular truss

3.3.1 Overview

The next shape analyzed is the standard rectangular truss shown in Figure 14. This bridge-typology truss has a constant span of 40m and 4 partitions. W = 10m, as it is the length of one partition which is the space between two vertical members. H is the variable height of the truss. Similar to the triangular truss, P = 117kN. Thus, it is possible to find the forces in the truss members as a function of H/W. Once the forces are found, the members can be sized according to Figure 8 and the GWP can be calculated. The members are split into four groups: vertical, top, bottom and diagonal. These 4 groups are each assigned one of two materials: steel or timber with 16 total combinations. The material combinations are referred to in the order "Vertical - Top – Bottom – Diagonal" with "s" denoting steel and "g" denoting glulam. For example, "s-g-s-g" means that the vertical and bottom members are steel while the top and diagonal members are glulam.

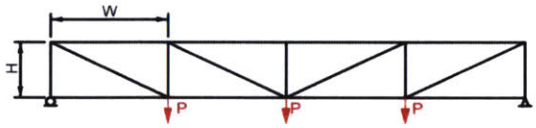

Figure 14: Standard Rectangular Truss design for a bridge typology

3.3.2 Results

The data in Figure 15 and Figure 16 is for the standard rectangular bridge truss shown in Figure 14 with $0.1<H/W<2.6$. They show the material combinations grouped into four clusters, sorted by their vertical and top members. The vertical and top members are the compression members of the truss, while the bottom

and diagonal members are in tension. These compression members, depending on the *H/W* ratio, have a large influence in the GWP. In contrast, the tension elements make little difference regardless of the *H/W* ratio. When $H/W<0.7$, there are two clusters only dependent on the top member. This can be seen in Figure 16a, which shows the GWP contribution for each member type per material when $H/W= 0.5$. Though all materials decrease when changed to glulam, the top members have a significantly higher contribution for both materials. When $0.8<H/W<1.4$, there are four clusters dependent on both the vertical and top members. In Figure 16b, when $H/W = 1.0$, the vertical members are now making a comparable contribution. In Figure 15, at $H/W=1$, the w-s-X-X and s-w-X-X cross as the top member begins to control the GWP. When $H/W>1.5$, the data reverts back into two main clusters dependent only on the vertical member material. This dependency is shown in Figure 16c. Even though there is often a common assumption that compression members behave better in glulam, depending on the *H/W* ratio, a compression member's material may not make a difference in the GWP. Similarly, the common assumption that tension members behave better in steel has shown to be insignificant for these conditions. Also shown in Figure 15 are *H/W* ratios that result in the minimum GWP for each material combination. While all minimum GWP values have *H/W* ratios between 0.6 and 1.0, each of the four clusters varies slightly. For example, all of the "g-s-X-X" minimums are at $H/W = 1.0$, while the "s-g-X-X" minimums are either 0.6 or 0.7. This means that the shape of the optimal solution depends on the specific material choices.

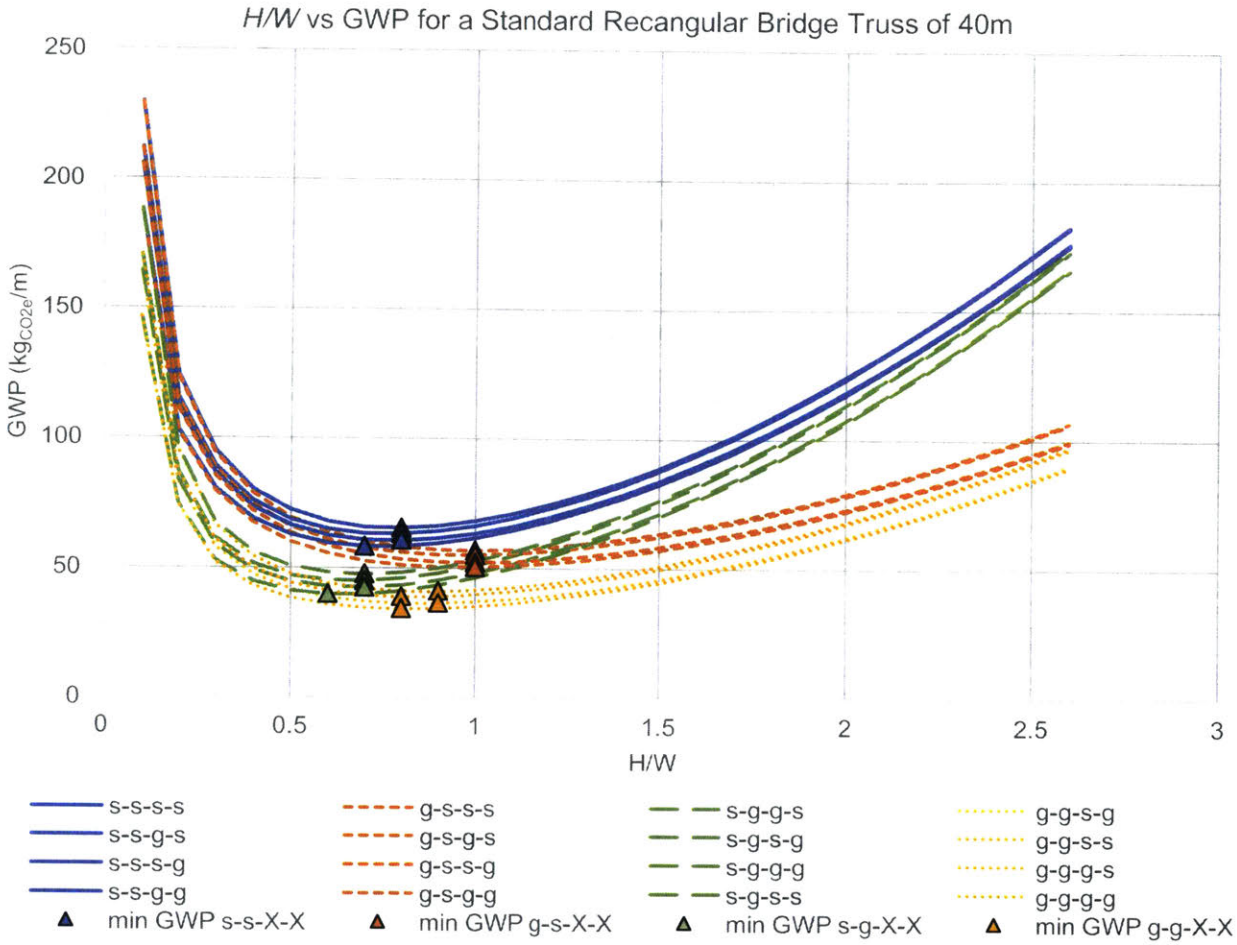

Figure 15: The GWP for varying H/W ratios of a standard rectangular bridge truss of 40m for all 16 material combinations (Material Order: Vertical-Top-Bottom-Diagonal)

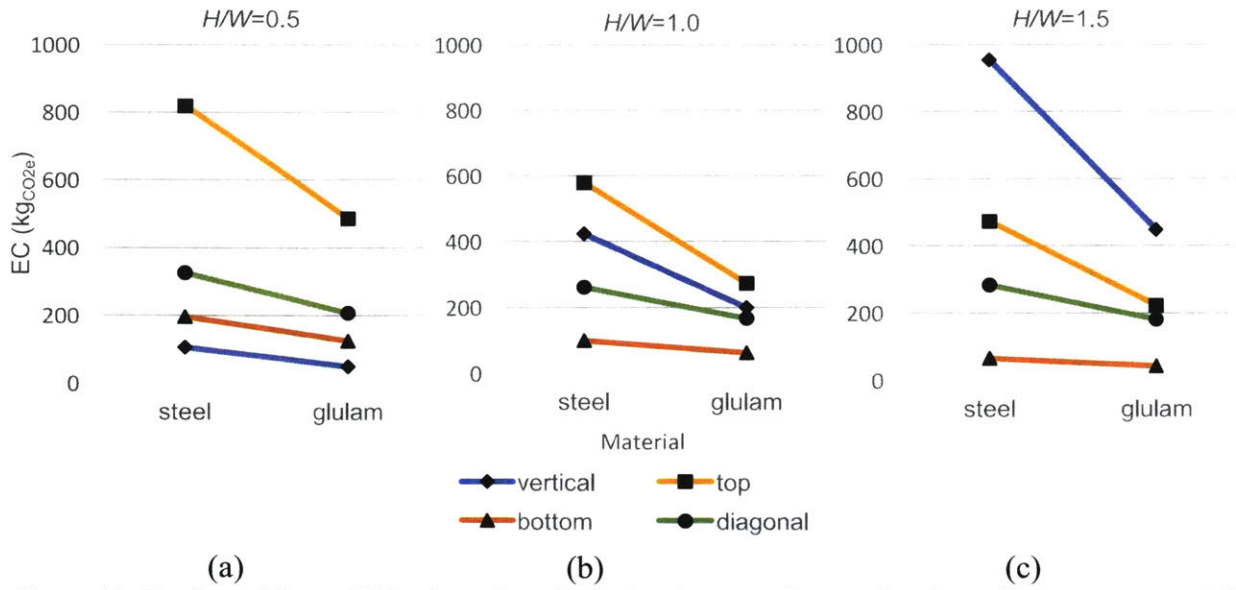

Figure 16: For three different H/W values, the embodied carbon contribution of each member type per material option

3.3.2 Sensitivity Analysis

The sensitivity analysis explores the effects on the GWP by changing the ECC and strength properties of the materials. These changes are listed below in Table 2. Each row in the table is an independent change and, aside from the change listed in that row, all other properties are the same as in Table 1. Figure 17 shows the results when changing the material properties by looking at the minimum GWP for each material combination for $0.1<H/W<2.6$. When the steel ECC is raised to 2.03 and the vertical and top members are steel, the GWP is high. However, once glulam is added for one or both of these groups, the GWP decreases. When the timber ECC value is raised to 0.87, the minimum GWP for each material combination stays relatively constant. As a result, these two lines cross each other in Figure 17. Increasing the steel stress has little effect on the minimum GWP values. In Figure 18, the same data is now sorted by the property change on the x-axis, instead of the material combination. This graph shows how the spread of data changes. When the steel stress increases, the four clusters based on the vertical and top members become more distinct. When the steel ECC increases or the glulam ECC decreases, these clusters become less distinct. When the glulam ECC value is high, one large cluster forms, meaning that every material combination yields a similar GWP.

Table 2: Sensitivity Analysis Changes

Material being changed	Change	Notes
Steel	Fy = 34.5 kN/cm^2	Higher Strength Steel
Steel	ECC = 2.03 [4]	35.5% recycled rate
Timber	ECC = 0.87 [4]	Includes biomass (not from a sustainably managed forest)
Timber	ECC = 0.09 [20]	Includes carbon sequestration, landfill at end of life

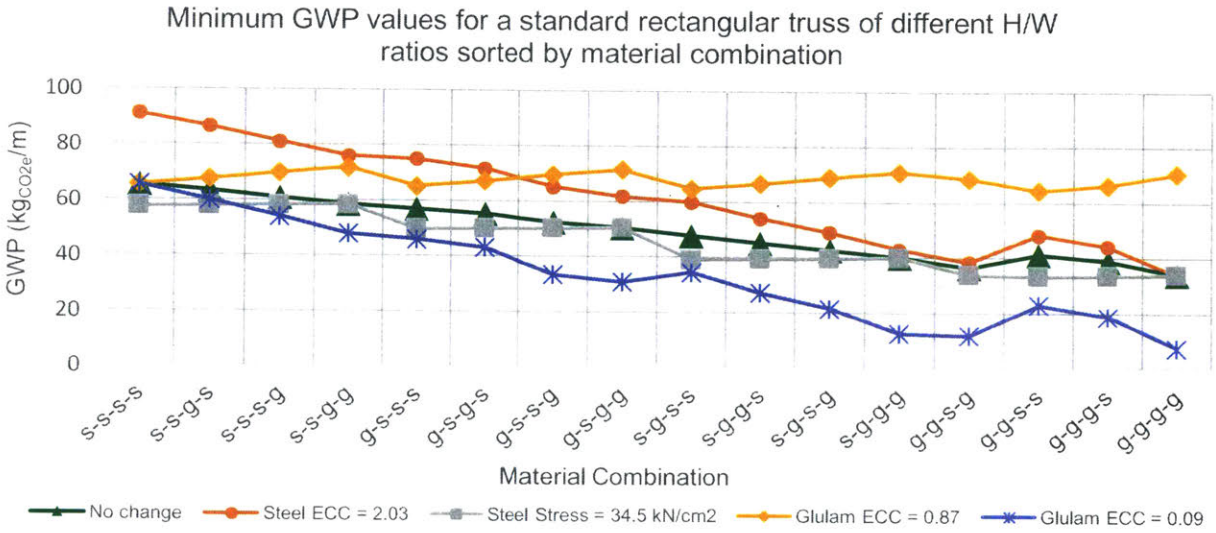

Figure 17: Sensitivity Analysis on how changing the material properties affects the GWP, sorted by material combination (Material Order: Vertical-Top-Bottom-Diagonal)

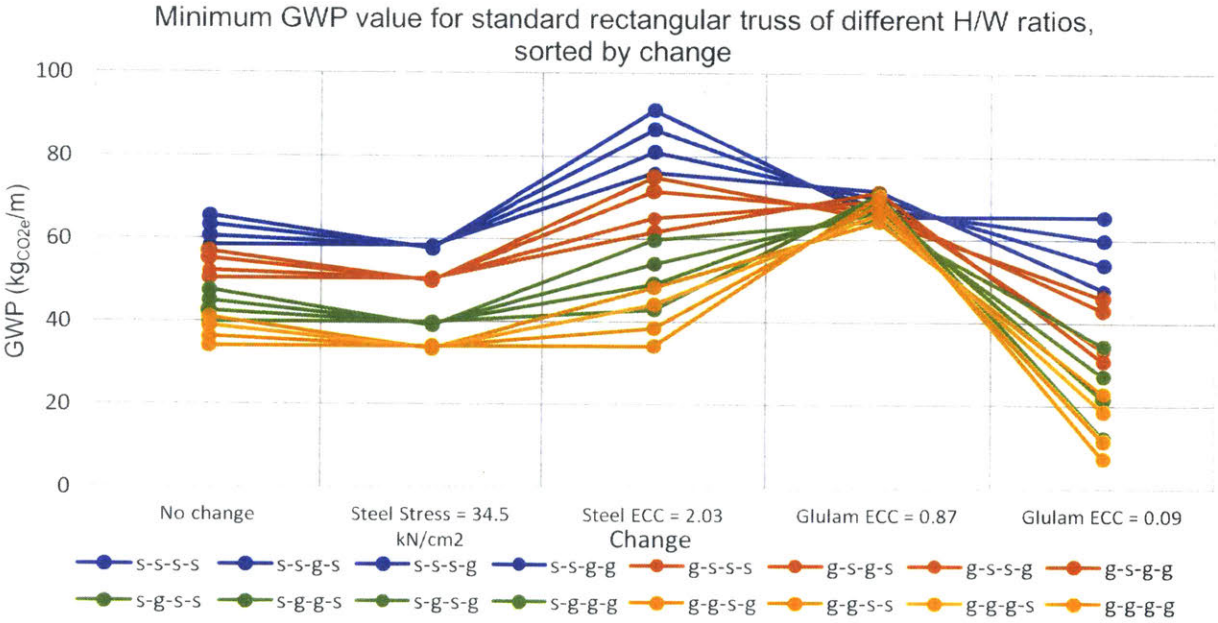

Figure 18: Sensitivity Analysis on how changing the material properties affects the GWP, sorted by the property change (Material Order: Vertical-Top-Bottom-Diagonal)

3.4 Key results

These results show that, while glulam can be a useful material due to its low density, its lower strength means that glulam designs will not always be the least-weight option. However, its lower ECC can allow for less carbon-emitting structures. Nonetheless, this is dependent on which members are being substituted with glulam. Not all substitutions will result in a significant drop in the GWP. The compression members were often more influential in the lowering the GWP when switching to glulam instead of steel. Different ECC values for steel and glulam affected which material combinations could result in the lowest GWP. In contrast, changing the strength value of steel had little effect.

4. Grasshopper Optimization and Calculations

In addition to hand calculations, it is useful to consider numerical analysis and optimization methods in order to study more complex structural types and shapes. This chapter expands the analysis of the previous chapter using a parametric programming environment (Grasshopper) with an integrated finite element analysis and cross section sizer (Karamba) and a numerical optimization tool (Goat). The chapter focuses specifically on medium- and long-span simply supported planar trusses. The first section gives an overview about the Grasshopper set up and the constraints in the design. The next section discusses the optimization process. The third section shows how the results are comparable to the hand calculations in Section 3. The fourth section shows the results and the final section discusses key contributions.

4.1 Overview

Two truss types are considered: bridge and roof. For the bridge design, the supports are at the bottom members, while for the roof design, the supports are at the top members. These are shown in the top and bottom pictures of Figure 19, respectively.

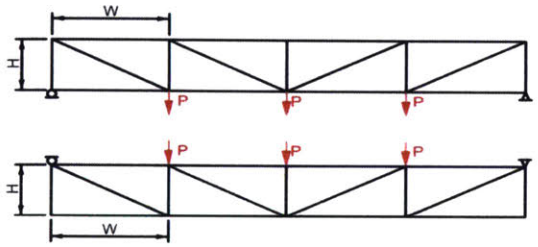

Figure 19: Standard Rectangular Truss design for bridge (top) and roof (bottom) typologies

A constant loading method was used for all analyses. The load P, in kN, is calculated in equation 1 shown below. This is equivalent to an applied load of approximately 9.6-11.7kN/m, based upon the number of partitions.

$$P = \frac{8.8 * \text{Span [m]}}{\text{Number of Partitions} - 1} \quad (1)$$

This calculation method analyzes the truss using Grasshopper with Karamba, a linear elastic finite element analysis plug-in [5, 21]. For each design, three different spans are analyzed. The bridge design uses full spans of 20m, 35m, and 50m while the roof design uses spans of 15m, 30m, and 40m. These lengths were chosen because they are typical span lengths for each type. Unlike the previous truss designs, this calculation method does not require the truss to stay in its rectangular shape. The truss is formed by a non-uniform rational B-spline (NURBS) curve. This curve is formed by control points and the ranges of their x and y coordinates are determined by the span length and the height/full span ratio, which is kept constant at 0.125. Setting the x and y coordinates to their maximum values yields the standard rectangular truss in Figure 19. The NURBS curve is then divided into sections of equal horizontal length based on the number of partitions and the points at these divisions are connected to the neighboring nodes with lines to mimic a Pratt truss. For the roof design, the NURBS curve forms the bottom chord nodes; while for the bridge design, the curve forms the top chord nodes. A bridge design is shown in Figure 20.

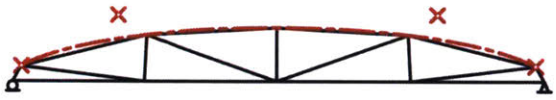

Figure 20: Creating the Grasshopper truss using a NURBS curve (shown in the dashed red line)

Karamba is used to solve for the forces in the trusses and to size the members using a component called Optimize Cross Section [5]. The steel members are hollow tubes and the glulam members are solid squares as shown in the images of Figure 8. The module finds the smallest possible cross section from one of two lists, one for steel and one for timber, depending on the given material. The radii for the steel members range from 1cm to 50cm in increments of 1cm, and the edge lengths for the glulam members range from 6cm to 104 cm in increments of 2cm. Using the preset Karamba material properties, steel was of the "S335" type and glulam was of the "(VH)III" type [5]. These properties are comparable to values in Table 1.

4.2 Grasshopper optimization details

Goat, another plugin for Grasshopper, is used for shape optimization. The variables in the shape optimization are the coordinates of the control points for the NURBS curve and the number of partitions. Due to 16 material combinations and 6 span lengths, a total of 96 optimizations are run on the Grasshopper script. Goat, which uses the NLopt library, has several different optimization algorithms, including DIRECT, BOBYQA, and Sbplx [22]. For each of the 96 combinations, the optimization is run as described in Figure 21. The global optimizer is used first to narrow the design space closer to the global minimum and the local optimizers are used to refine that design to a solution with an even lower GWP. Switching back and forth between the two local algorithms allows the solution from each algorithm to be used as the initial condition for the other, allowing for a more accurate optimization. Each combination is run twice to ensure accuracy.

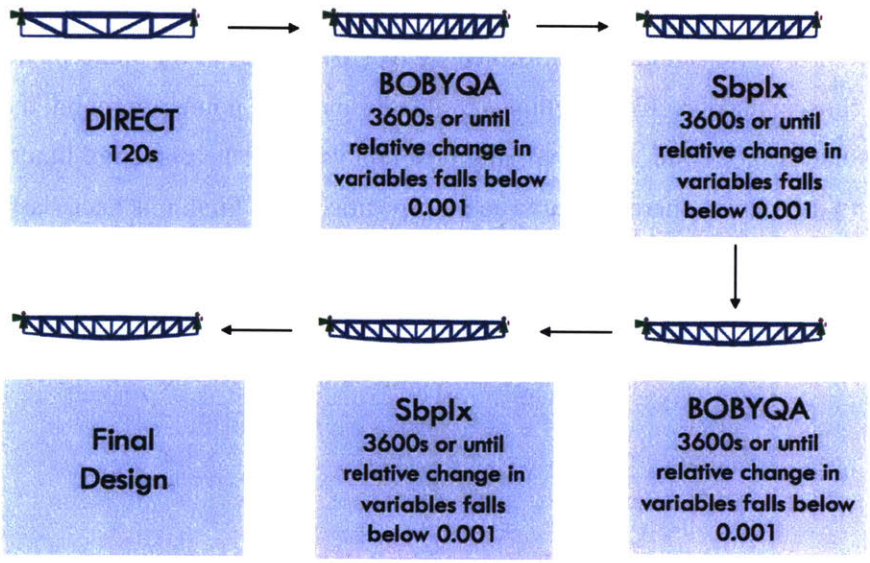

Figure 21: Flow chart for optimization process

DIRECT is a global deterministic solver. It was originally presented by Jones *et al.* in 1993 [23]. It divides the design space into smaller and smaller boxes using the Lipschitz continuity condition. A function is Lipschitz continuous if equation 2, for some constant K, is true [24]. Thus, a lower bound for f(x) can be found as shown in equations 3 and 4, for a two-dimensional function [24]. If this lower bound is found for every box, the box with the lowest lower bound is divided into smaller boxes [23]. However, in the DIRECT process, K is unknown. As a result, for any value of $0<K<\infty$, DIRECT divides all boxes where the function

has the lower bound [23]. While it is possible to prove that the global optimum will always be found after a sufficiently long time, it can often be found after only a few iterations of dividing the rectangles [23].

$$|f(x) - f(x')| \leq K|x - x'|, \forall x, x' \in D \tag{2}$$

$$X(a, b, f, K) = \frac{a+b}{2} + \frac{f(a)-f(b)}{2K} \tag{3}$$

$$B(a, b, f, K) = \frac{f(a)+f(b)}{2} - \frac{K(b-a)}{2} \tag{4}$$

BOBYQA is a local quadratic approximations solver that Goat can run. If the quadratic approximation is Q(x), then Q(y_j)=F(y_j) for j = 1, 2, ...m [25]. The y_j points are chosen and adjusted and m is a constant. The model is updated by minimizing the Frobenius norm of the change to the second derivative matrix of Q [25].

The final algorithm used was Sbplx, a local subplex Nelder-Mead variant. Nelder Mead starts with a simplex, a structure in n-dimensional space formed by n+1 points not in the same plane [26]. Once the simplex points are chosen, the objective function is evaluated and three points are found: the set of variables that produce the worst (x_w), second worst (x_l), and best (x_b) value of the objective function [26]. Using these three points, five different operations are run in a specific order. First, it is necessary to calculate the average of all the points excluding the worst, shown in equation 5 [26]. The five possible operations are shown in equations 6-10 [26]. They are manipulated as described in the *Stanford University: Introduction to Multidisciplinary Design Optimization* notes [26]. Sbplx uses Nelder-Mead on a sequence of subspaces [22].

$$x_a = \frac{1}{n} \sum_{i=1, i \neq w}^{n+1} x_i \tag{5}$$

Reflection:

$$x_r = x_a + \propto (x_a - x_w) \tag{6}$$

Expansion:

$$x_e = x_r + \gamma(x_r - x_a) \tag{7}$$

Inside contraction:

$$x_c = x_a - \beta(x_a - x_w) \tag{8}$$

Outside contraction:

$$x_c = x_a + \beta(x_a - x_w) \tag{9}$$

Shrinking:

$$x_i = x_b + \rho(x_i - x_b) \tag{10}$$

4.3 Validation of Grasshopper results

Figure 22 compares the Grasshopper and spreadsheet results for the 16 material combinations for a standard rectangular truss with *H/W* = 2.6 and Span = 40 m. The reason that the Grasshopper data has a higher GWP for each material combination is because the spreadsheet sizes the members using the minimum required cross section from a continuum. However, the Grasshopper script uses a set list of cross sections, described in 4.1, and finds the smallest possible cross section from that list based on the minimum required size. Both results are similar, showing the accuracy of the Grasshopper script.

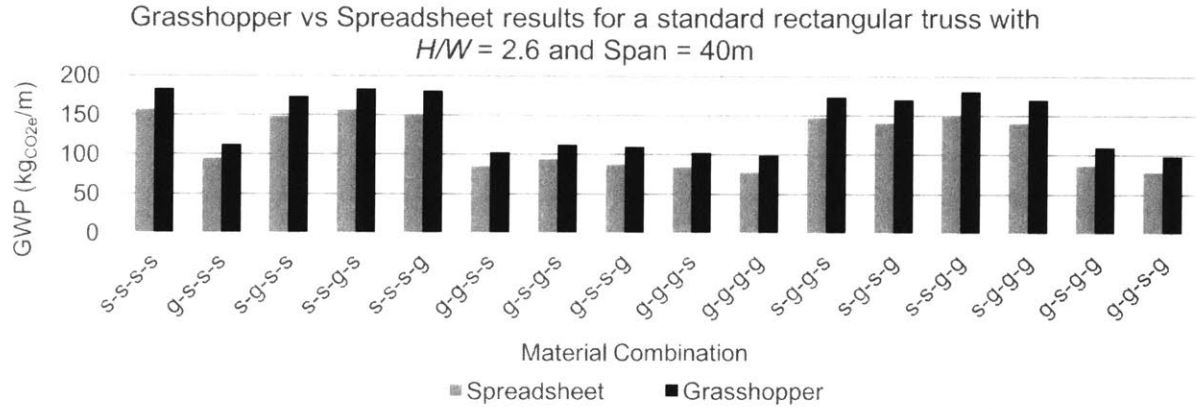

Figure 22: The Grasshopper and Spreadsheet results for a standard rectangular truss are close to each other, showing the accuracy of the Grasshopper script (Material Order: Vertical-Top-Bottom-Diagonal)

4.4 Grasshopper results

4.4.1 Best and worst performing optimized designs

Figure 23 and Figure 24 show the best and worst optimized designs for each span length respectively. The all-steel trusses were not the worst performing for any of the designs. Many of the designs, including the other 84 not pictured, displayed a similar shallow arch shape and the optimal number of partitions for designs was often between 8 and 12. The rest of the 96 optimized designs can be found in the Appendix.

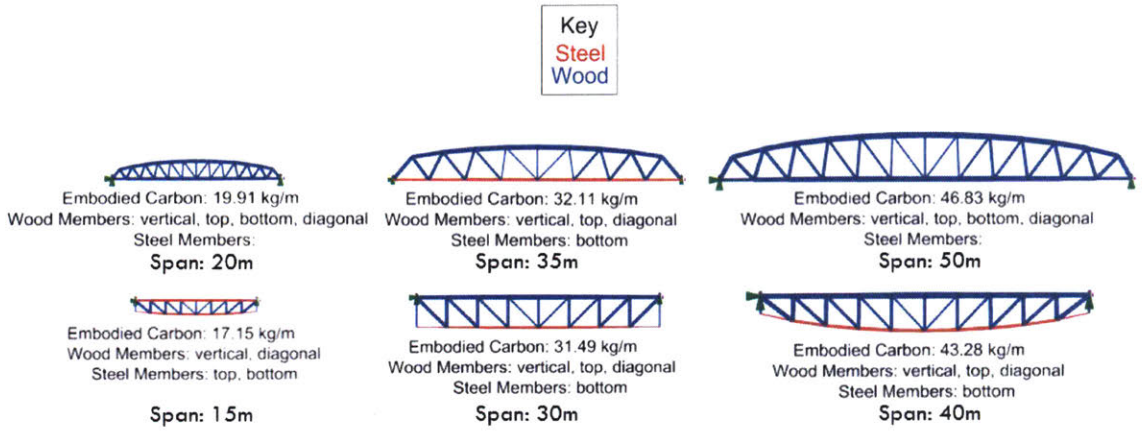

Figure 23: The minimum GWP design for each span length

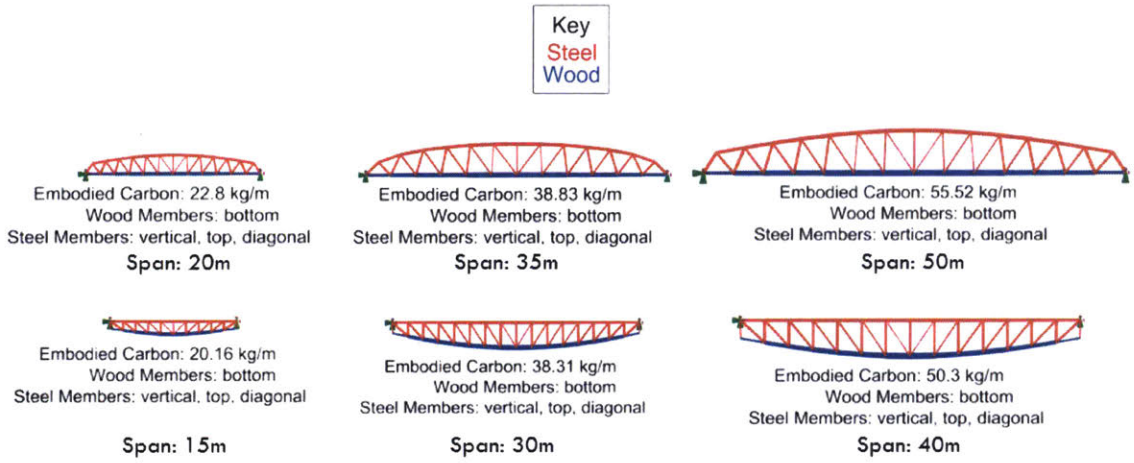

Figure 24: The maximum GWP design for each span length

All the maximum GWP designs have steel for all members except the bottom chord ("s-s-g-s"). In contrast, many of the minimum GWP designs are the reverse, "g-g-s-g". The 35m spans of these combinations, s-s-g-s and g-g-s-g, are compared in Figure 25, Figure 26, and Figure 27 for their volume, weight, and GWP per member cluster. Figure 25 shows that the glulam members, for either design, have a larger volume than their steel counterparts due to a larger required cross sectional area. For the vertical and diagonal clusters, this may also be attributed to the g-g-s-g having 4 additional partitions. Thus, even though glulam is less dense than steel, the glulam members are still heavier than their steel counterparts. However, when looking at the GWP in Figure 27, the GWP for the vertical, top, and bottom clusters for the s-s-g-s design are greater than those for the g-g-s-g design. In this case, the glulam bottom and diagonal members are both heavier and less sustainable than a steel option. In contrast, even though the glulam vertical and top members are the heavier options, the high ECC value for steel causes the GWP for the steel options to be higher. The g-

g-s-g design weighed 2085kg and had a GWP of 32.11 kg_{CO2e}/m whereas the s-s-g-s design weighed less, 1730kg, but had a GWP of 38.83 kg_{CO2e}/m. In this case, the design with more glulam was heavier, but more sustainable.

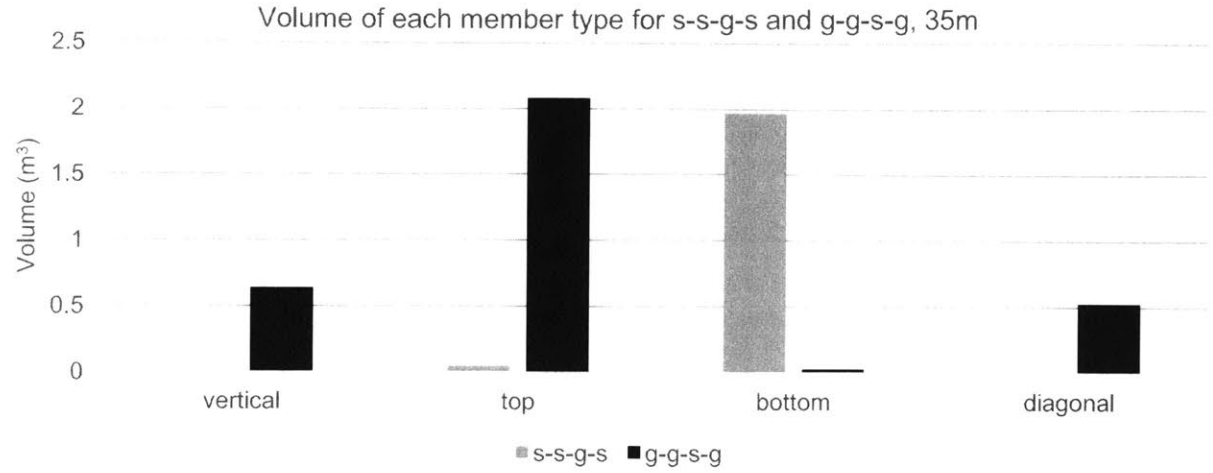

Figure 25: The volume of each member type for 35m spans of s-s-g-s compared to g-g-s-g

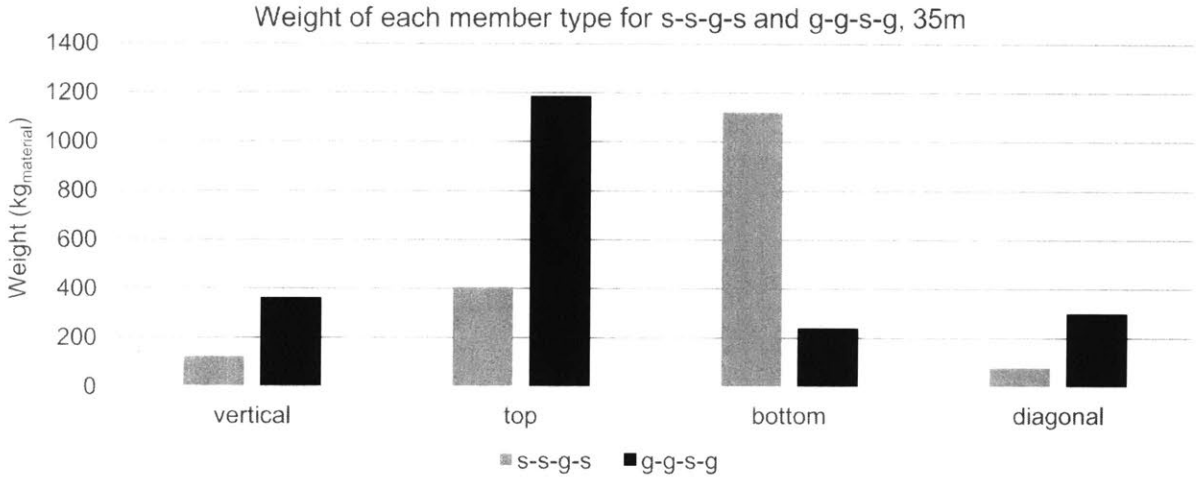

Figure 26: The weight of each member type for 35m spans of s-s-g-s compared to g-g-s-g

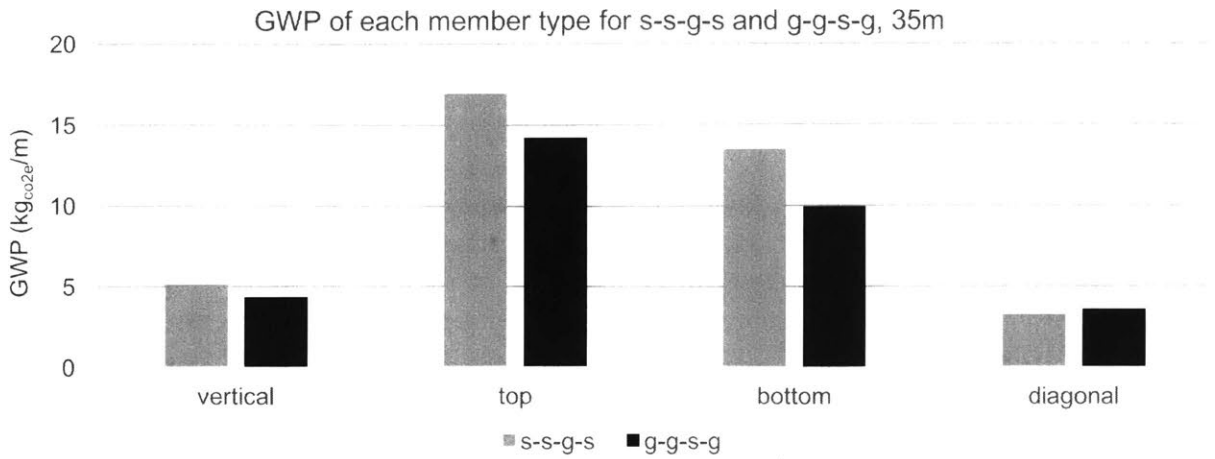

Figure 27: The GWP of each member type for 35m spans of s-s-g-s compared to g-g-s-g

The best performing 15m design, as shown in Figure 23, has both the top and bottom members in steel ("g-s-s-g"). In this design, the vertical and top members are in compression and the bottom and diagonal members are in tension. This design is compared to g-g-g-g in Figure 28 -Figure 31. This all-glulam design has the same members in compression and tension, although it has two extra partitions. Figure 28 shows an image of the 15m span of g-g-g-g while Figure 29, Figure 30, and Figure 31 compare the volume, weight, and GWP, respectively, for each member cluster. The vertical and diagonal members are both made of glulam. The all-glulam design has slightly higher values for these members for the volume, weight, and GWP; however, this can most likely be attributed to the extra partitions which require extra vertical and diagonal members. The top and bottom members, which differ in material, have vastly different volumes and weights for the different designs. In the truss images, the member widths are scaled to the cross-sectional area. When compared to the g-s-s-g design, all the members of the g-g-g-g designs, particularly the top and bottom members, are thicker. This is because glulam requires a much larger cross-sectional area. Even though glulam is less dense than steel, this larger cross sectional area causes the all-glulam structure to be heavier. Even though the steel top member option is lighter than the glulam option, the higher steel ECC value results in the steel option having a higher GWP. However, for the bottom members, the steel option is light enough that the higher steel ECC value does not cause the steel option to have a higher GWP. Therefore, for three out of four of the member types, the GWP for the all-glulam design is greater than the g-s-s-g design and, thus the total sum of the GWP for all-glulam is greater. The g-s-s-g design weighed 315kg and had a GWP of 17.15 kg_{CO2e}/m whereas the g-g-g-g design weighed 639kg and had a GWP of 17.89 kg_{CO2e}/m. In this case, the all-glulam design was twice the weight and had a slightly higher GWP than the g-s-s-g design.

Embodied Carbon: 17.89 kg/m
Wood Members: vertical, top, bottom, diagonal
Steel Members:

Figure 28: All-wood 15m optimized truss

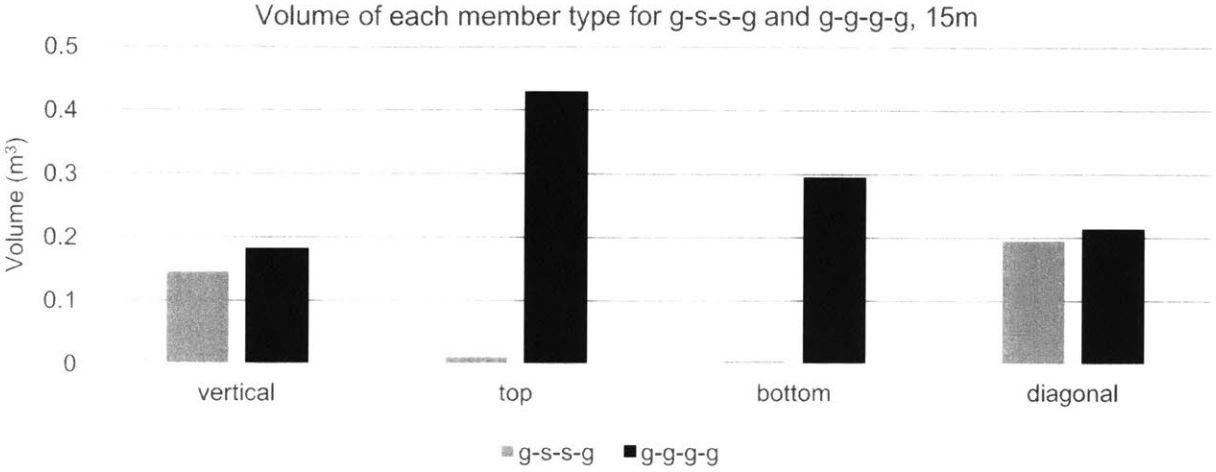

Figure 29: The volume of each member type for 15m spans of g-s-s-g compared to g-g-g-g

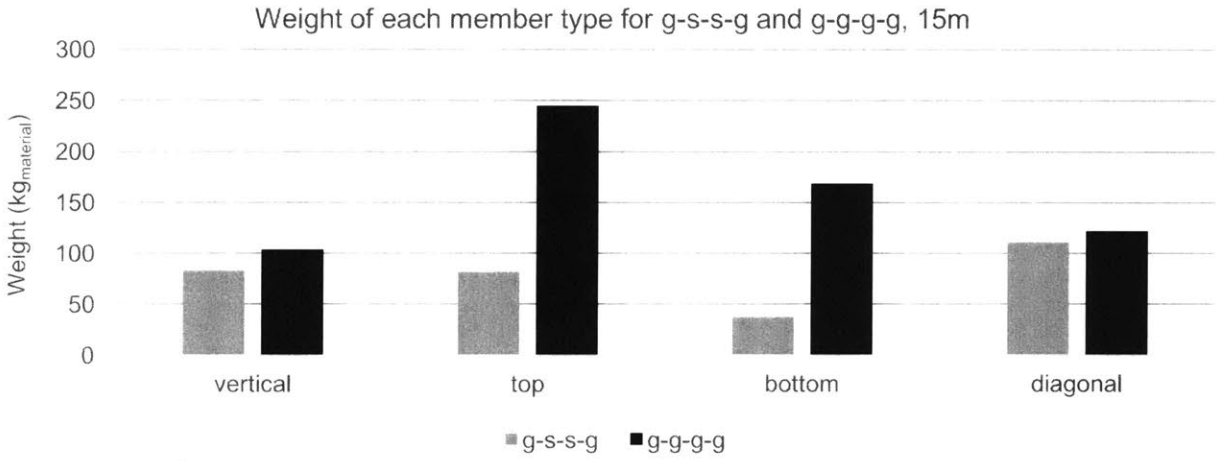

Figure 30: The weight of each member type for 15m spans of g-s-s-g compared to g-g-g-g

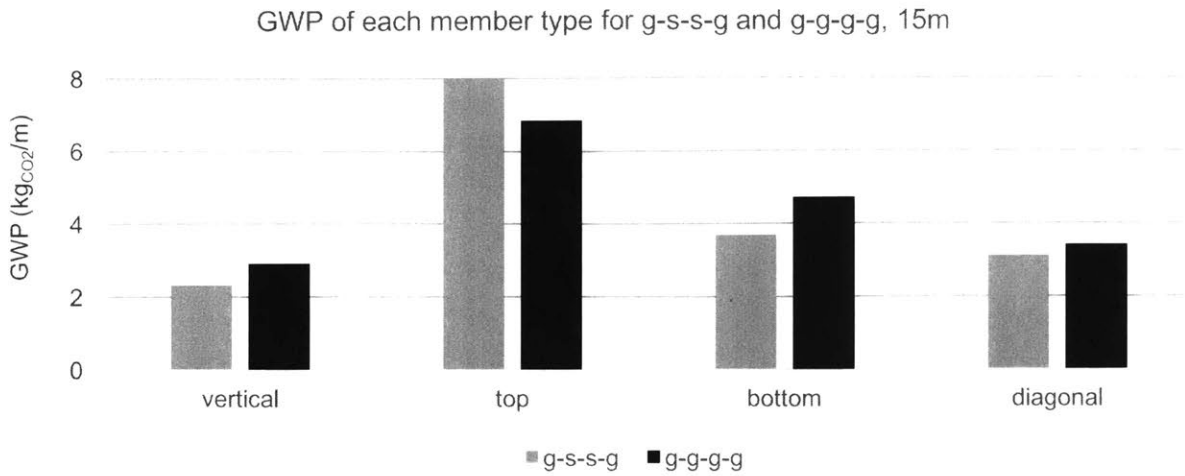

Figure 31: The GWP of each member type for 15m spans of g-s-s-g compared to g-g-g-g

4.4.2 Overview of the 96 optimized designs

Figure 32 shows all 96 designs for span vs. GWP. For many of the spans, the all-wood and all-steel designs were not the best and worst performing, respectively. For the larger spans, the spread of data is greater and, within each span, there is a more distinct separation of the material combinations based upon vertical and top member materials. The trusses with glulam for both these members performed best while those with steel performed the worst. However, as the spread gets smaller as the span decreases, this trend is less noticeable. Figure 33 sorts these same results by material combination for each span from highest to lowest GWP. Switching from the worst to best design from each span yielded savings of approximately 15-22%. The lower spans, 15m and 20m, have the four clusters (s-s-X-X, s-g-X-X, g-s-X-X, g-g-X-X) mixed. For 15m, "g-g-g-s" even has a slightly higher GWP than "s-s-s-s". When the span increases, the 35m bridge design begins to show separation by vertical and top members with all four "s-s-X-X" designs ranked highest and all four "g-g-X-X" designs ranked lowest. While the 30m roof design shows a little more separation between these designs, "g-g-g-s" is still ranked higher than "s-s-s-g". For the last set of spans, 40m and 50m, the clusters become more distinct. The 50m span shows that the "s-s-X-X" and "g-g-X-X" clusters have the worst and best GWPs respectively.

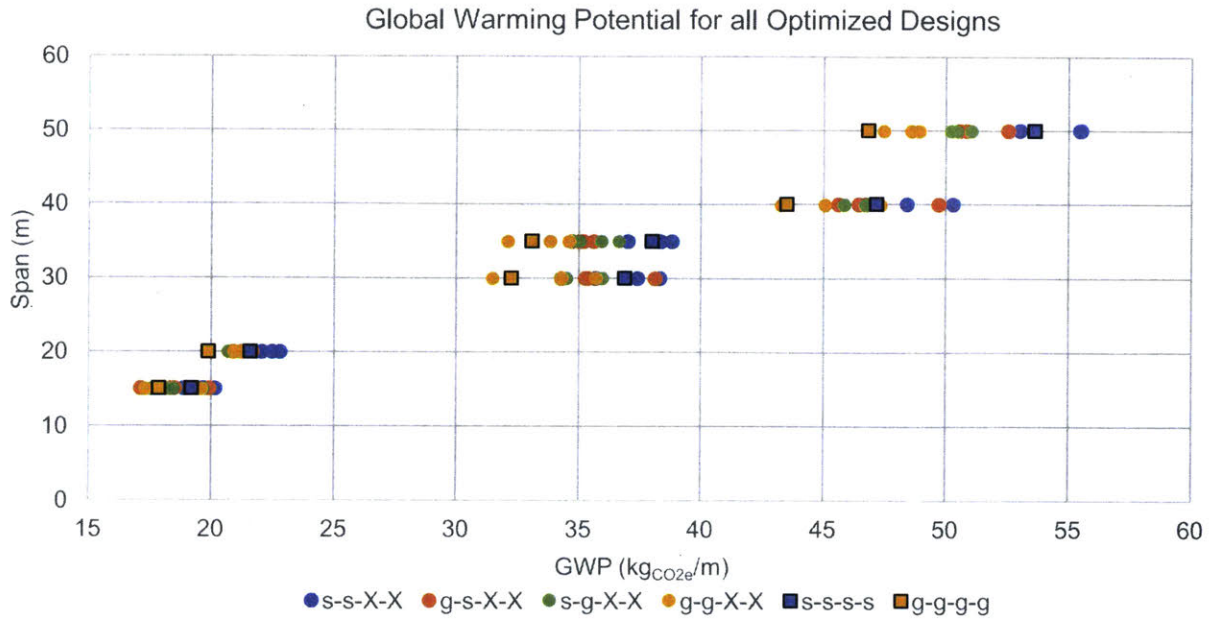

Figure 32: The GWP for all optimized designs for each material combination for each span (Material Order: Vertical-Top-Bottom-Diagonal)

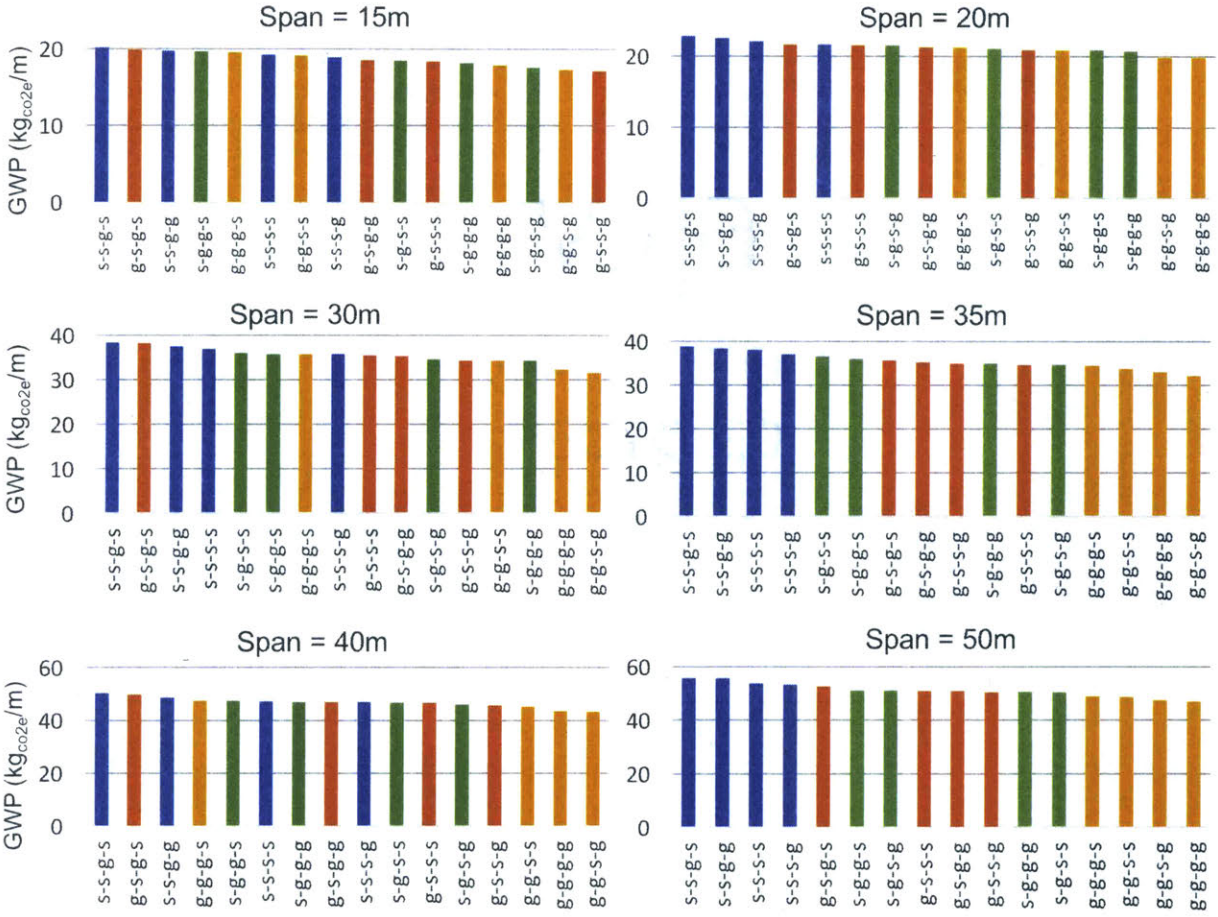

Figure 33: Material Combination vs GWP per span

The 40m roof span still does not show such distinct clusters as the 50m bridge design shows. For 40m, "g-g-g-s" increased its GWP ranking to the 4th highest, higher than "s-s-s-s". Even though these designs have different vertical, top, and bottom member materials, their GWP difference is only 0.17 kg_{CO2}/m. Alternatively, "g-g-g-s" and "g-g-g-g" differ only by the diagonal member material, yet the all-glulam GWP 3.85 kg_{CO2}/m lower. Figure 34 shows images of these two material combinations and Figure 35-Figure 37 explores the data from the two material combinations more in depth for volume, weight, and GWP. The volume and weight for the steel diagonal cluster is much less than those made of the glulam. However, the high ECC value for steel causes the steel diagonal to have a higher GWP. Even though the diagonal members are changing material, the vertical members, which remain glulam in both designs, are the largest increase in GWP when switching to "g-g-g-s". There are also two more vertical partitions in "g-g-g-g" then "g-g-g-s", which can contribute to the greater weight. In this example, the 40m g-g-g-g design weighed 4141 kg and had a GWP of 43.49 kg_{CO2e}/m whereas the g-g-g-s design weighed 3924 kg and had a GWP of 47.34 kg_{CO2e}/m. In this case, the heavier structure, all-glulam, was more sustainable.

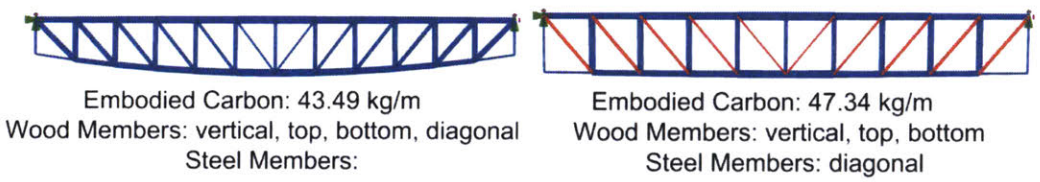

Figure 34: 40m designs for g-g-g-g (l) and g-g-g-s (r)

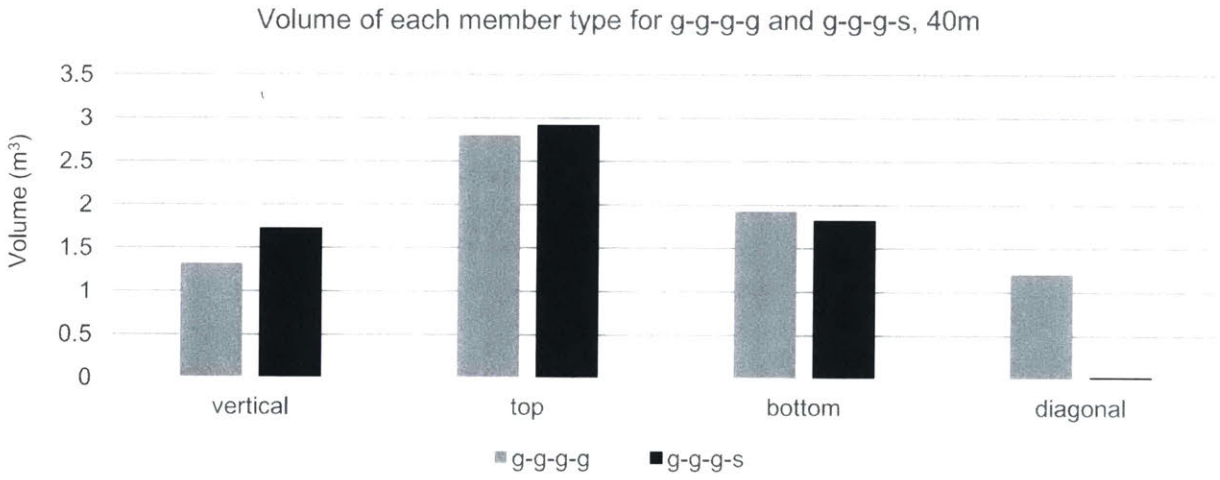

Figure 35: The volume of each member type for 40m spans of g-g-g-g compared to g-g-g-s

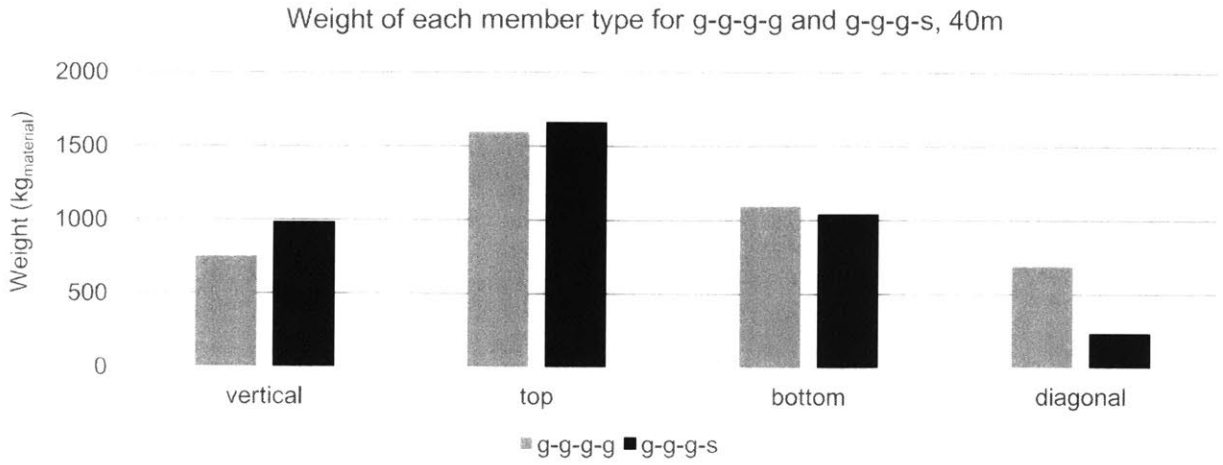

Figure 36: The weight of each member type for 40m spans of g-g-g-g compared to g-g-g-s

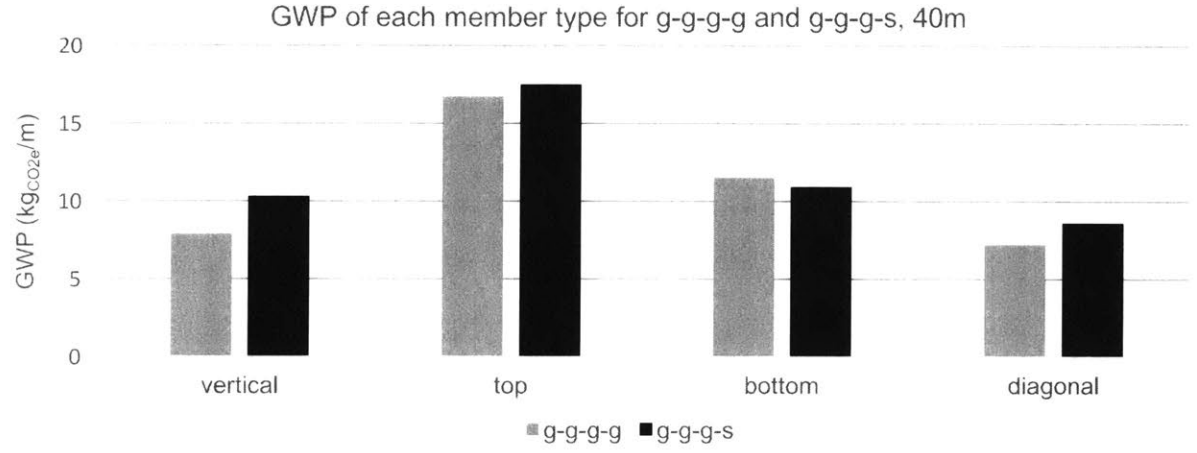

Figure 37: The GWP of each member type for 40m spans of g-g-g-g compared to g-g-g-s

Figure 38 compares each optimized design to the standard rectangular truss of the same span length and material combination within Grasshopper. It plots the percentage of GWP savings from using optimization and indicates the maximum and minimum material combinations for each span. Both truss types show that as the span increases, the spread is larger and there is greater potential for more savings through optimization. However, the bridge spans (20m, 35m, and 50m) show a smaller spread and greater potential for savings compared to the roof designs. Figure 39 and Figure 40 show the same data sorted by the material combination for the roof designs and bridge designs, respectfully. Figure 38 shows that designs for minimum and maximum percent savings were of the "X-g-X-X" and "X-s-X-X" designs, respectively. However, Figure 39 shows that, for the roof typology, every material combination is sorted by this clustering. That is, all the roof designs with steel as the top member had greater savings after optimization than the designs for that span length with glulam as the top member. Figure 40, which shows this data for the bridge designs, does not show this relationship as drastically, particularly for the 20m span.

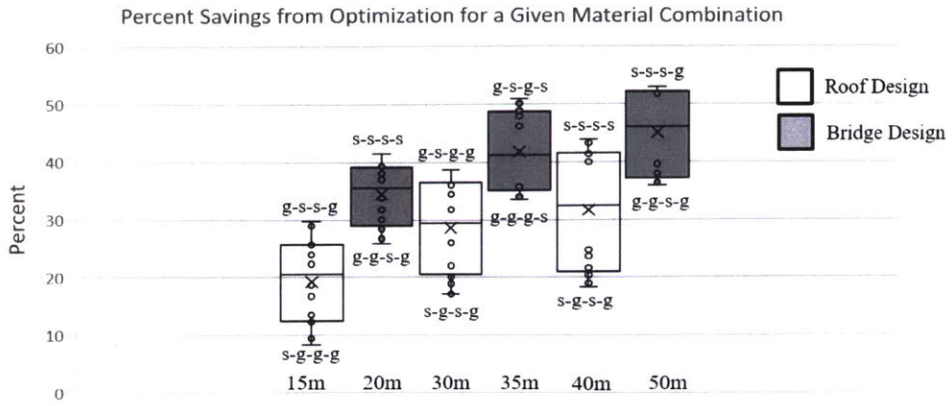

Figure 38: The percentage of GWP savings from optimization compared to the standard rectangular truss for each material combination, sorted by span length (Material Order: Vertical-Top-Bottom-Diagonal)

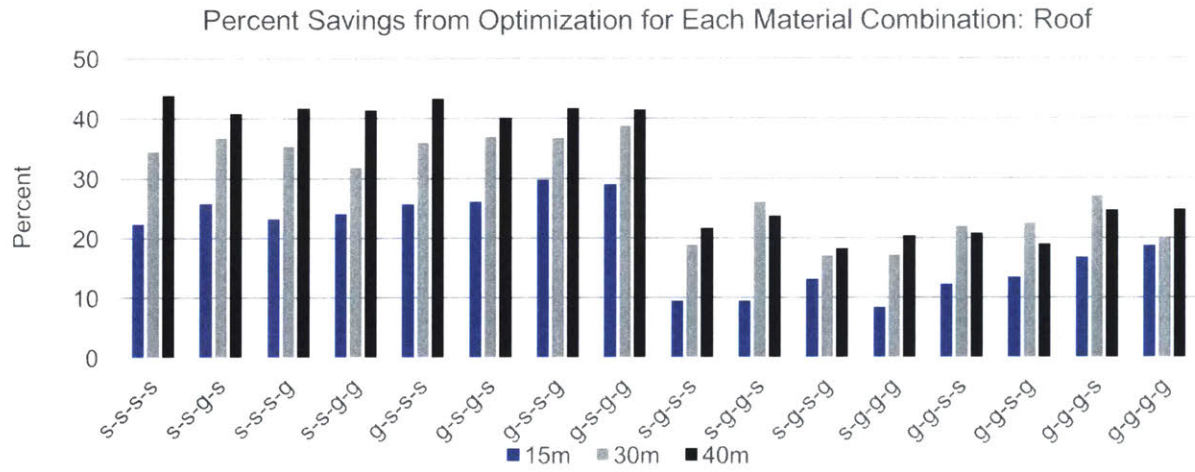

Figure 39: The percentage of GWP savings from optimization compared to the standard rectangular truss, sorted by material combination, for the roof designs (Material Order: Vertical-Top-Bottom-Diagonal)

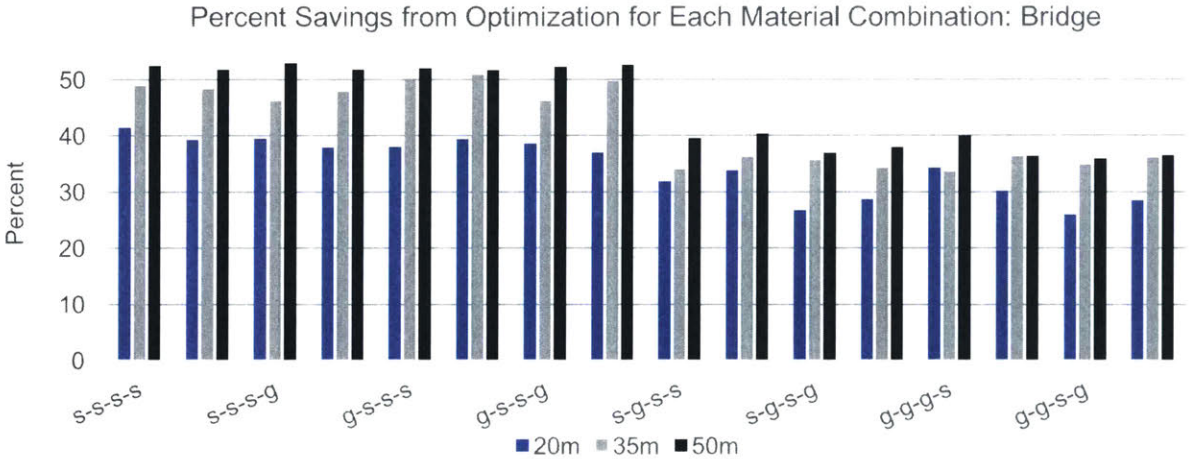

Figure 40: The percentage of GWP savings from optimization compared to the standard rectangular truss, sorted by material combination, for the bridge designs (Material Order: Vertical-Top-Bottom-Diagonal)

Figure 41 - Figure 46 explore the percent savings compared to the all-steel standard rectangular truss for each span length for two different design cases. The first case keeps the standard rectangular shape but changes the material combination while the second case performs shape optimization for the new material combination. In the first case, for most of the bridge designs, little to no savings were found if the top member was steel; however, when the top member was glulam, 12-35% of GWP could be saved for a standard rectangular truss design. This relationship is also true for the roof designs.

For the 20m bridge span in Figure 41, the designs that could save the most just by changing some of the materials to glulam, but keep the rectangular shape, were also the designs with the maximum savings after optimization. All of the 20m spans saved 38-46% after optimization compared to the all-steel standard rectangular truss. While significant savings can be made through shape optimizations, even greater savings can be made through finding an optimal material combination in conjunction with the optimization. For a 35m all-steel truss, shown in Figure 42, it is possible to save 49% of GWP just through shape optimization; however, substituting all but the bottom members for glulam ("g-g-s-g") and optimizing will yield savings of 57% compared to the all-steel rectangular truss. Likewise, only 6% of GWP can be saved by using a standard rectangular g-s-g-g truss instead of an all-steel rectangular truss; yet, optimizing the g-s-g-g- truss can yield savings of 53% compared to the all-steel rectangular truss. Optimizing a 50m truss, shown in Figure 43, with glulam diagonal elements and steel for all others ("s-s-s-g") can lead to GWP savings of 53% compared to the all-steel rectangular truss. For this s-s-s-g design, only 0.01% of the GWP could be saved if the standard rectangular design is used.

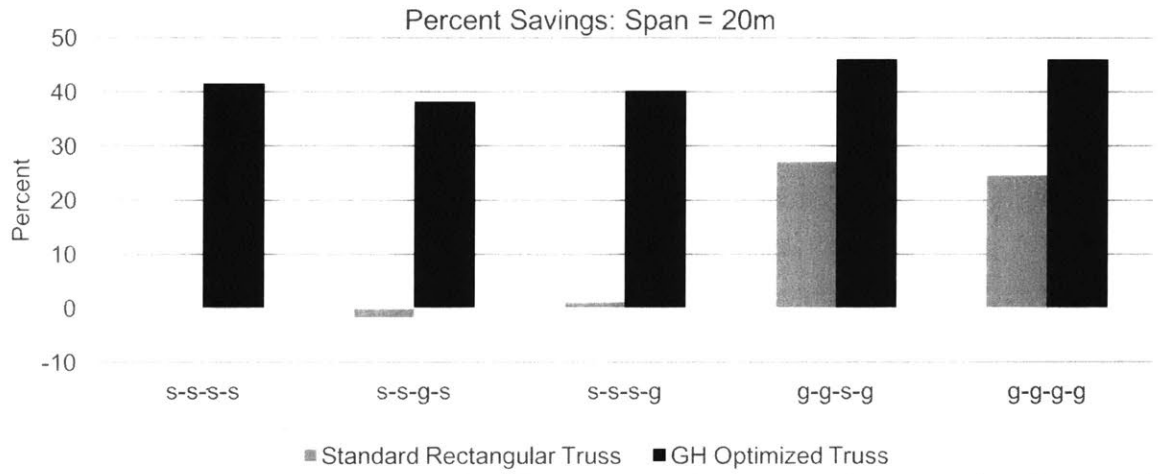

Figure 41: Percent savings of GWP compared to all steel rectangular truss for select material combinations, 20m

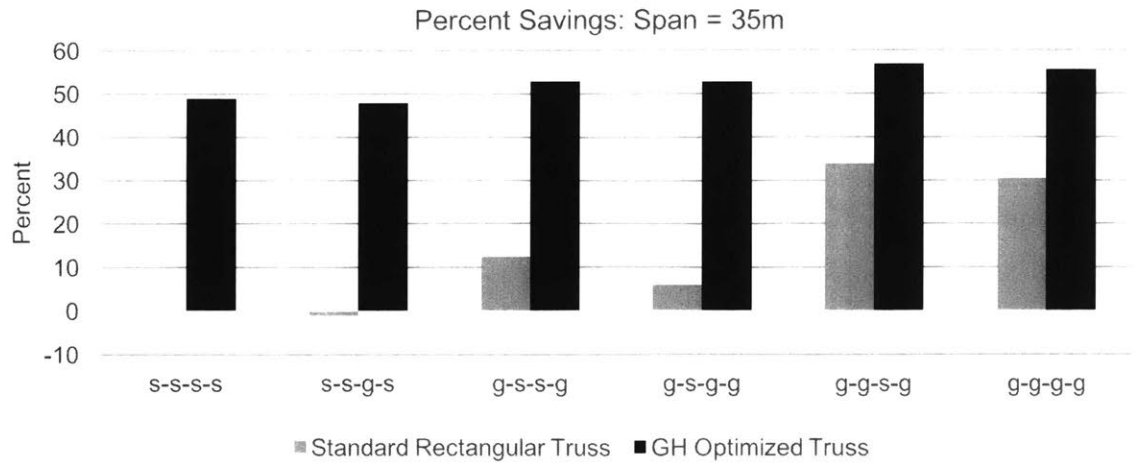

Figure 42: Percent savings of GWP compared to all steel rectangular truss for select material combinations, 35m

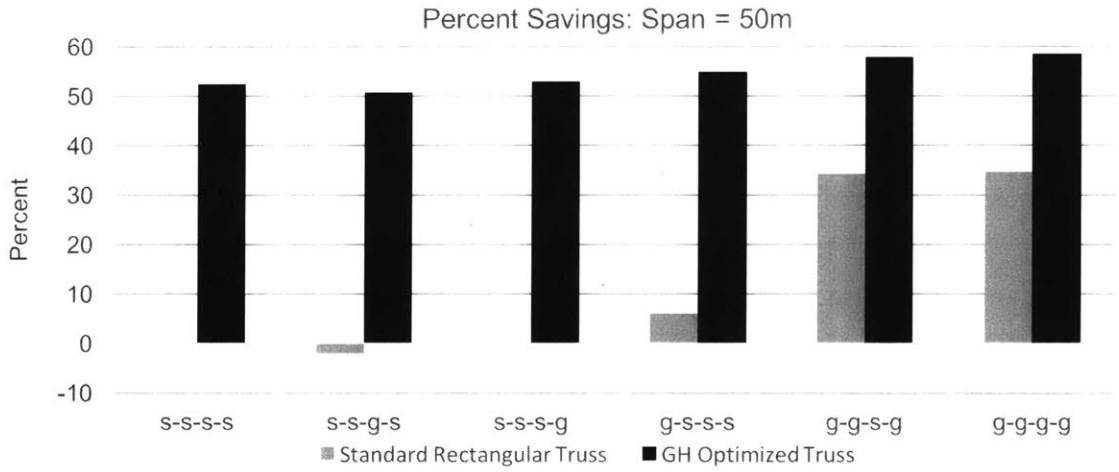

Figure 43: Percent savings of GWP compared to all steel rectangular truss for select material combinations, 50m

Figure 44 explores these results for a span of 15m. When changing some of the members of the rectangular truss to timber, the GWP can increase; however, when the optimization is run, all optimized designs perform better than the all-steel rectangular truss. For the standard rectangular g-s-s-g design, the GWP is only improved by 1% compared to the all-steel rectangular design. However, after shape optimization, g-s-s-g has the maximum savings, 31%, of all material combinations. Figure 45 shows this data for a 30m span. An interesting comparison is between the g-g-s-g and g-g-g-s designs. When looking at the material savings for the standard rectangular truss shape, they save 28% and 13%, respectively. After shape optimization, they increase to 44% and 37%, respectively. In these designs, both compression member clusters and one tension cluster use glulam while the other tension cluster uses steel. However, which tension cluster is steel makes a difference in the possible savings. The percent savings for the 40m span is shown in Figure 46. One interesting comparison can be made between the g-s-g-g and s-g-s-s material combinations, which have the opposite material for each cluster. For the standard rectangular truss, only 5% savings can be

reduced by switching from all-steel to g-s-g-g, while 29% can be saved by using the s-g-s-s design. However, after shape optimization, these material combinations have similar savings, approximately 44% each.

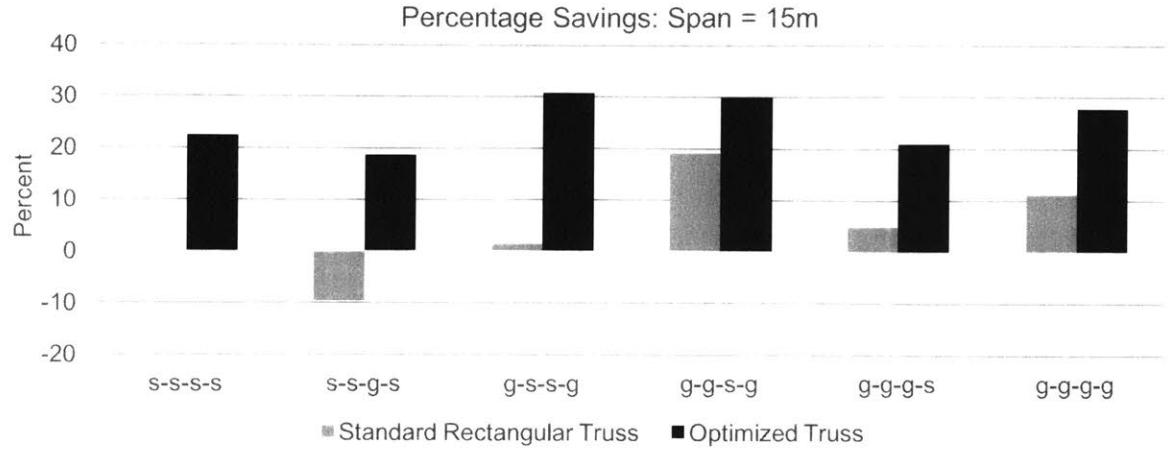

Figure 44: Percent savings of GWP compared to all steel rectangular truss for select material combinations, 15m

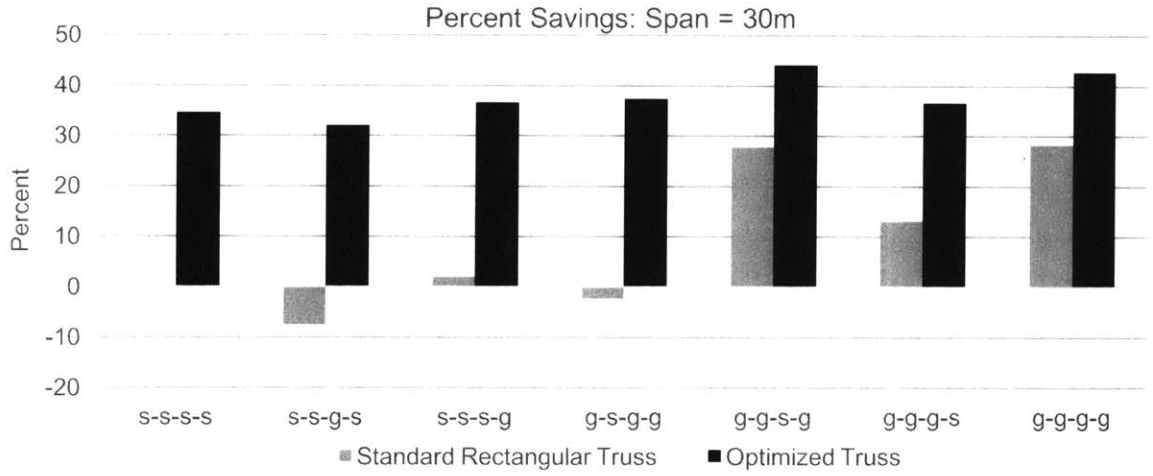

Figure 45: Percent savings of GWP compared to all steel rectangular truss for select material combinations, 35m

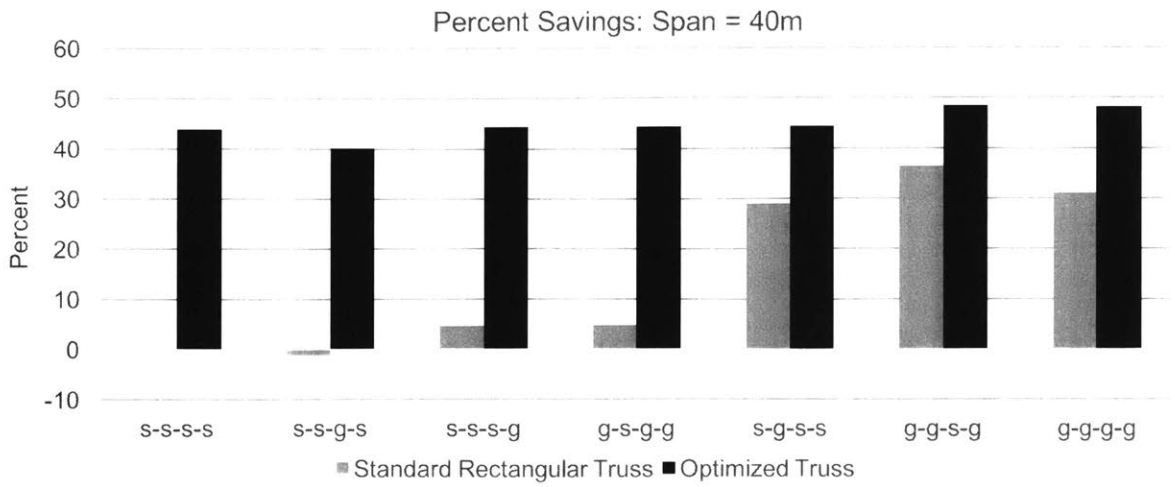

Figure 46: Percent savings of GWP compared to all steel rectangular truss for select material combinations, 40m

4.5 Key results

These results show the advantages of shape optimization in conjunction with material optimization. Although one material combination may result in the lowest GWP for the standard rectangular truss design, this same material combination will not necessarily have the lowest GWP of the 16 material combinations after optimization. Likewise, those combinations that show few, and sometimes negative, savings for the standard rectangular truss design, can result in some of the highest savings after optimization. How much savings is possible and how much of an effect the material combination can have on these savings are dependent on the span length. Depending on the span length and topology, the material of both the tension and compression members can have a major influence on the GWP. Grasshopper and Goat allow for more complex designs than the spreadsheet analysis and these results show that with parametric form finding tools, it is possible to find more sustainable geometries.

5. Conclusion

5.1 Summary of contributions

This thesis presents the first multi-material truss optimization for embodied carbon. While previous research has been done on structural optimization, embodied carbon, and sustainability comparisons between materials, there has yet to be comprehensive research on the combination of all three. Structural optimization has been used in truss structure design since the 1960s, yet it often focuses on weight minimization, which, as this thesis has shown, does not necessarily correlate to GWP minimization. This is because steel, while it is a denser material than glulam and emits more carbon dioxide per unit weight, is a stronger and stiffer material. This can result in a smaller required cross sectional area and, potentially, a lower weight or GWP. While an emphasis on sustainable design in the built environment has grown, most work focuses on reducing the operational carbon. The work that is on embodied carbon focuses on quantifying ECC values for different materials and benchmarking existing designs. This thesis demonstrates potential advantages of multi-material design when trying to reduce the embodied carbon emissions in the design of new structures.

This thesis first investigates a simple triangular truss section as well as a standard rectangular truss. It analyzes how the importance of the material for each member cluster changes as the H/W ratio changes. A sensitivity analysis is also conducted on the results to show how changing different material properties can change the importance. The thesis then uses Grasshopper and a plugin, Karamba, to analyze more complex multi-material trusses. Another Grasshopper plugin, Goat, is used for the optimization of these trusses.

These optimized results are compared to the standard rectangular trusses of the same material combination to show the advantages of optimization. They are also compared to the all-steel standard rectangular truss to show the advantages of multi-material design.

5.2 Key results

The results show that multi-material truss optimization can have a large impact on reducing the embodied carbon in truss structures. An all-wood shape-optimized 15m span roof truss has savings of 28% compared to an all-steel rectangular truss. However, when substituting the top and bottom members with steel and running the optimization process, the savings increase to 31%. For a 35m all-steel truss, it is possible to save 49% of GWP just through shape optimization; however, substituting all but the bottom members for glulam and optimizing will yield savings of 57% compared to the all-steel rectangular truss. Optimizing a 50m truss with glulam diagonal elements and steel for all others can lead to GWP savings of 53%. For a standard rectangular truss, the materials of the compression members have a greater impact on the GWP than the tension members. These results show that shape-optimization is a useful tool when looking to reduce the embodied carbon and multi-material designs, in combination with this optimization, can lead to even more savings.

5.3 Potential impact

Architects and engineers can use these results as a guide when designing their own sustainable truss structures, which may contain different spans, shapes, and ECC values than the ones used in this thesis. Though the exact results cannot be copied due to the specific constraints of every unique project, these results will encourage designers to explore optimization tools and multi-material designs and not necessarily revert to substituting steel members with timber with the assumption that the design will become more sustainable. Other truss topologies or structural systems may yield different results. Multi-material designs have been built before in large structures such as the Scottish Parliament in Figure 4 as well as in smaller-scale structural systems such as open web joists shown in Figure 5. With more attention to the embodied carbon in these designs, more sustainable structures can be built. Figure 47 shows a rendered example of the 35m g-g-s-g design. It has a GWP of 32.11 kg_{CO2e}/m, the lowest of the 35m material combinations.

Figure 47: A rendered example of the 35m g-g-s-g design

5.4 Limitations and future work

One of the limitations of this work is the assumption that all joints and connections are feasible. It assumes that all joints contribute to the GWP equally and can therefore be excluded from the GWP comparison. In addition, it is assumed that any truss structure is feasible to construct. One area of future research is to design the joints for the trusses and calculate the additional GWP. Another area to research further is the sensitivity analysis. As section 4 shows, the results are sensitive to ECC values. ECC values can vary because there are many factors involved in the calculation of the ECC for a material. Running the optimization process with different values will likely produce different results. Using different materials aside from timber or steel or analyzing a different structural system will also produce different results.

5.5 Concluding remarks

This research introduces a new approach for multi-material design optimization of embodied carbon and demonstrates the advantages of using multi-material designs for sustainability. The results show that simplistic assumptions about sustainable structural materials are not always valid, and that indeed a more nuanced and analytical approach to exploring multi-material solutions can often yield better results for reducing environmental impact.

References

[1] C. De Wolf, "Low Carbon Pathways for Structural Design: Embodied Life Cycle Impacts of Building Structures," Ph.D. dissertation, Dept. of Architecture, Massachusetts Institute of Technology, Cambridge, MA, 2017

[2] United States. "US Total Energy Statistics" *U.S Energy Information Administration,* 2016, [Online] https://www.eia.gov/energyexplained/?page=us_energy_home#tab3 [Accessed Apr 17 2018]

[3] P. Mayencourt and C. Mueller, Computational Design and Digital Fabrication of Timber Beams, 2017 [Powerpoint Slides].

[4] G. Hammond and C. Jones, "Inventory of Carbon and Energy," Sustainable Energy Research Team Mech Eng, Univ of Bath, UK 2011

[5] C. Preisinger, "Karamba User Manual for Version 1.2.2," *Karamba*, 2016

[6] *Steel Construction Manual,* American Institute of Steel Construction 15th ed., 2017

[7] M.F Ashby, "Materials and the Environment: Eco-informed Material Choice", Oxford, United Kingdom: Butterworth-Heinemann, 2012, 616p.

[8] P. Evans, "Scottish Parliament Debating Chamber" *Geograph,* Edinburgh, Great Britain, 2012 Available: http://www.geograph.org.uk/photo/2883793 [Accessed Apr 17 2018]

[9] O. Geiger, "Roundwood Open Web Joists", *Natural Building Blog*, Available: http://www.naturalbuildingblog.com/roundwood-open-web-joists/ [Accessed May 6 2018]

[10] "The Depot Gallery", *Architectural Timber and Millwork, Inc.,* Available: http://atimber.com/commercial-timber-work/ [Accessed May 6 2018]

[11] C. DeWolf, "database of embodied Quantity outputs," Available: https://www.carbondeqo.com [Accessed Apr 17 2018]

[12] F. Yang, "Embodied Carbon & Life Cycle Considerations in Building Structures". Walsh Seminar, ARUP, June 7-8 2016

[13] M. Trussoni; E. Simatic; C. Raebel; H. Huttelmaier. "Life Cycle Assessment Comparison for Long-Span Cable and Truss Structural Systems: Case Study" *J. Archit. Eng*, ASCE, pp 1-10. 2015

[14] Airports where the architecture soars. *Raleigh-Durham International (North Carolina)*. 2013. Available: http://www.cnn.com/2013/06/07/travel/airport-architecture-paul-goldberger/

[15] P Kripakaran; A. Gupta; J. Baugh. "A novel optimization approach for minimum cost design of trusses". *Computers and Structures 85,* pp 1782-1794. 2007

[16] N. Brown and C. Mueller, "Design for structural and energy performance of long span buildings using geometric multi-objective optimization," *Energy and Buildings 127.* pp 1-14, 2016

[17] M. Stolpe and K. Svanberg, "A stress-constrained truss-topology and material-selection problem that can be solved by linear programming." *Struct Multidiscipl Optim 27*(1), pp 126-129, 2004

[18] S. Rakshit, G. K. Ananthasuresh. "Simultaneous material selection and geometry design of statically determinate trusses using continuous optimization" Indian Institute of Science, 2007.

[19] R. Cazacu and L. Grama, "Steel Truss Optimization Using Genetic Algorithms and FEA", The 7th International Conference Interdisciplinarity in Engineering, Procedia Technology 12, p 339-346, 2014

[20] D. Weight, "Embodied through-life carbon dioxide equivalent assessment for timber products," *Institution of Civil Engineers: Energy Vol 164 Issue EN4.* Pp 167-182, Nov 2011

[21] "Grasshopper: Algorithmic Modeling for Rhino" 2018, [Online] Available: http://www.grasshopper3d.com/ [Accessed Apr 25 2018]

[22] NLopt Documentation, [Online] Available: https://nlopt.readthedocs.io/en/latest/ [Accessed May 6 2018]

[23] K. Ljungbergy, S. Holmgren, O. Carlborg, "Simultaneous search for multiple QTL using the global optimization algorithm DIRECT" *Bioinformatics 20(12)* Oxford University Press 2014,

[24] Y. Brise, "Lipschitzian Optimization, DIRECT Algorithm and Applications", 2008, Available: https://www.inf.ethz.ch/personal/ybrise/data/talks/msem20080401.pdf [Accessed May 6 2018]

[25] M.J.D. Powell, "The BOBYQA algorithm for bound constrained optimization without derivatives" *Centre for Mathematical Sciences Department of Applied Mathematics and Theoretical Physics, 2009* Available: http://www.damtp.cam.ac.uk/user/na/NA_papers/NA2009_06.pdf [Accessed May 6 2018]
[26]"Chapter 6: Gradient Free Optimization" *Stanford University: Introduction to Multidisciplinary Design Optimization* [Online] Available: http://adl.stanford.edu/aa222/lecture_notes_files/chapter6_gradfree.pdf [Accessed May 6 2018]

Appendix: All Optimized Designs

The following appendices show all 96 optimized designs. The layout of the grid is shown below. The order is "Vertical-Top-Bottom-Diagonal" with "s" denoting steel and "g" denoting glulam. The minimum and maximum GWPs for each span are outlined in black.

s-s-s-s	s-s-s-g	s-s-g-s
s-s-g-g	s-g-s-s	s-g-s-g
s-g-g-s	s-g-g-g	g-s-s-s
g-s-s-g	g-s-g-s	g-s-g-g
g-g-s-s	g-g-s-g	g-g-g-s
	g-g-g-g	

A. Span: 15m (Roof)

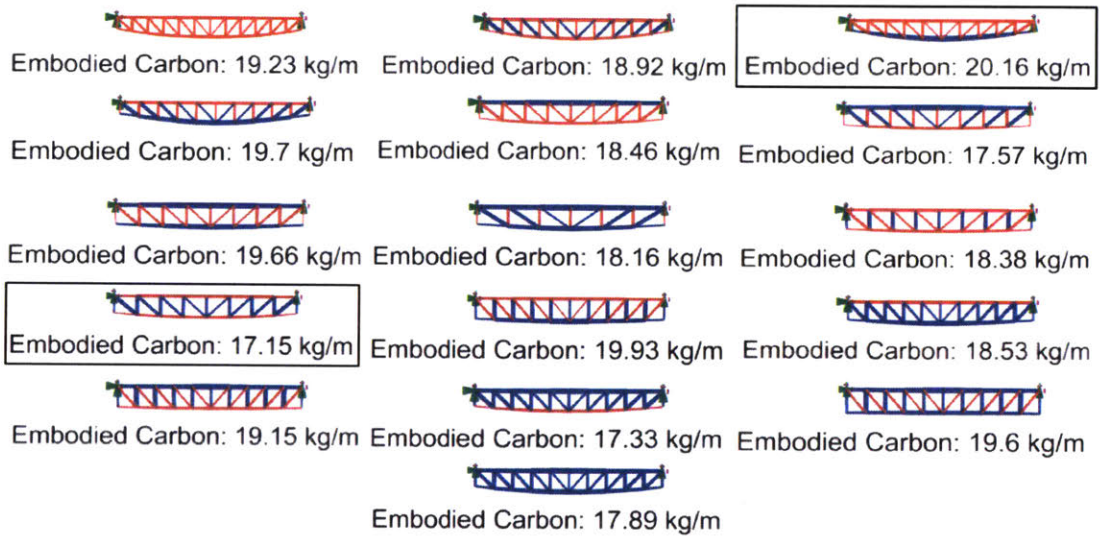

B. Span: 20m (Bridge)

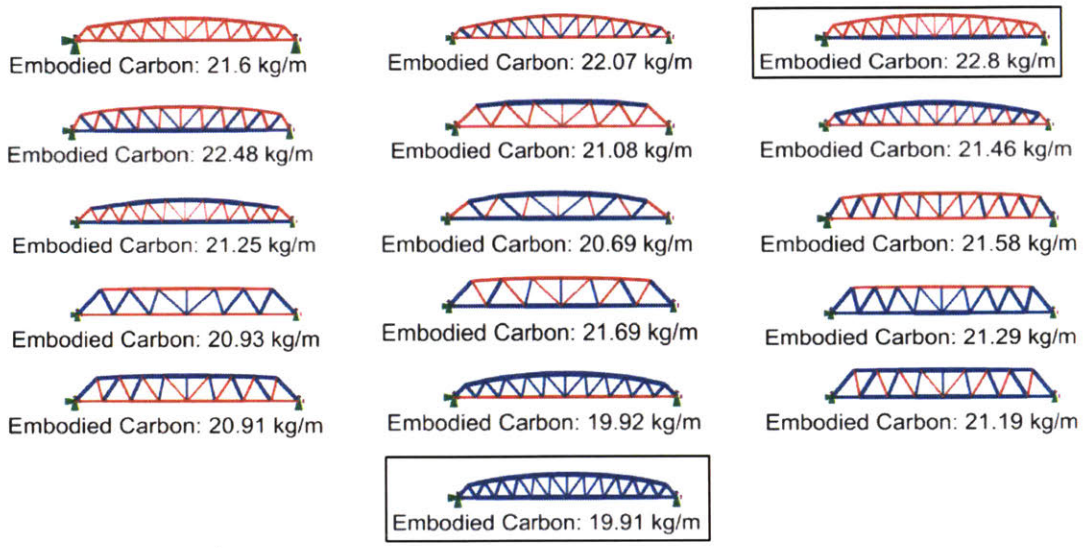

C. Span: 30m (Roof)

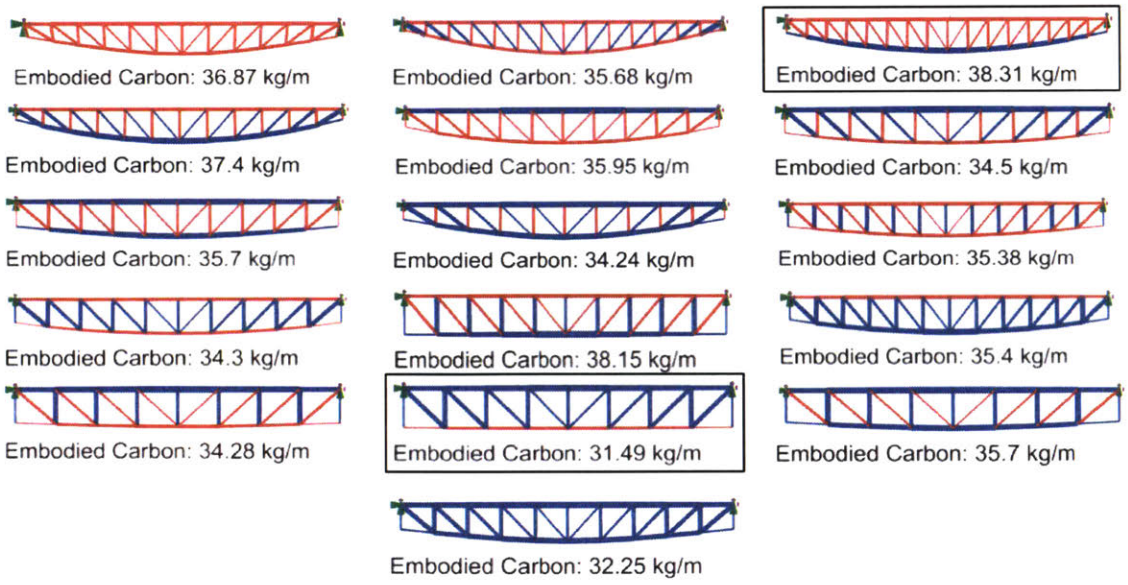

D. Span: 35m (Bridge)

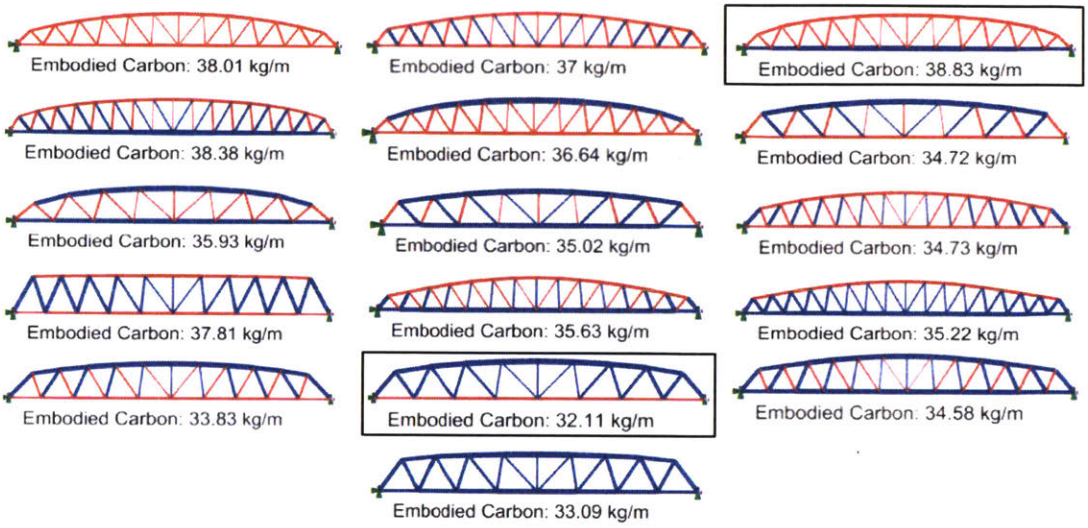

E. Span: 40m (Roof)

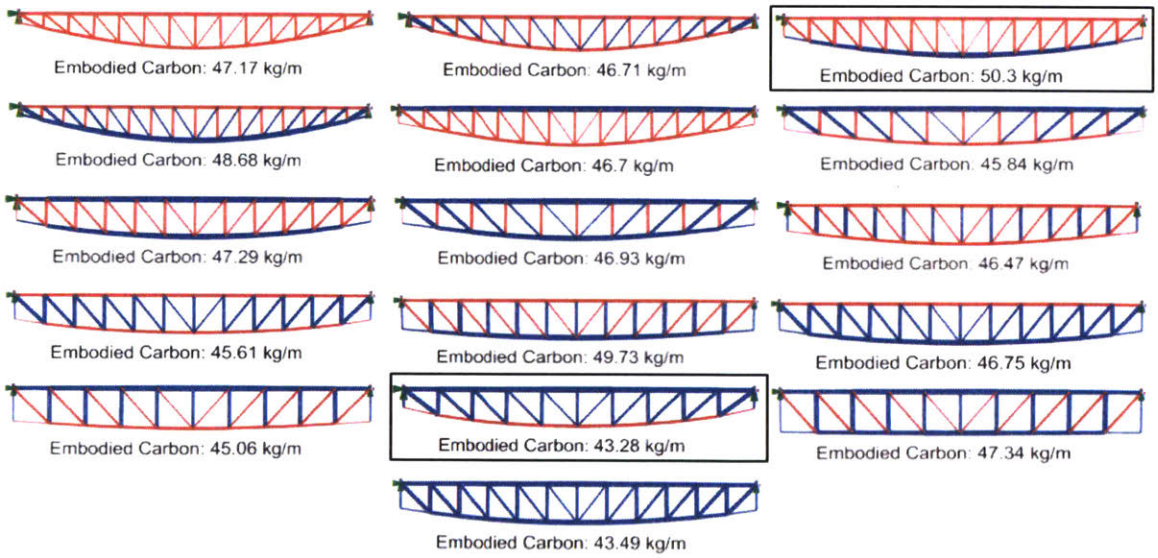

F. Span: 50m (Bridge)